UNIVERSITY OF TURKU

Inert Liquid Encapsulation: A Novel Approach to Enhancing Lifetime, Thermal Stability, and Recyclability of Solar Cells

Materials Engineering

Master's thesis

Department of Mechanical and Materials Engineering

Author:

Tommi Jokikyyny

23.2.2026

Turku

Statement of Originality

I hereby declare that the research, design, and experimental data presented in this thesis—specifically regarding the development of the "Prototype A" screw-based liquid module and the subsequent "Prototype B" refined ILE module—are my own original work.

The conceptualization of the Inert Liquid Encapsulation (ILE) system using dimethicone was initiated in early 2023. The experimental phase, including the documented nine-month outdoor aging tests in Turku, Finland, commenced on September 5, 2023. This thesis stands as the primary record of the invention and its subsequent development.

Master's thesis

Subject: Materials Engineering
Author: Tommi Jokikyyny
Title: Inert Liquid Encapsulation: A Novel Approach to Enhancing Lifetime, Thermal Stability, and Recyclability of Solar Cells
Supervisors: Prof. Kati Miettunen, Dr. Aapo Poskela
Number of pages: 43+11
Date: 23.2.2026

The decreasing dependence on fossil fuels amplifies the significance of renewable energy sources. Photovoltaics play a crucial role in the field, and the efforts to improve them have largely focused on enhancing efficiency. Little attention has been given to one of the most important components of solar modules: encapsulation.

Hence, the encapsulation of commercial solar modules has remained almost unchanged for decades, with the photovoltaic cell laminated into a crosslinked polymer material. This thesis presents a new way of encapsulating solar cells in inert materials that could significantly increase the lifetime of solar modules and facilitate easier recycling of the different components. This new encapsulation method paves the way for modular designs, with replaceable encapsulation materials and higher focus on the overall environmental impact of solar power. This thesis focuses on one main material while proposing other materials that pose wanted qualities. The material selected for the prototyping and experimental work was **dimethylpolysiloxane.**

Multiple prototypes were created, and the plausibility of the designs was tested in real life conditions during the harshest weather in Finland as well as in controlled laboratory conditions. Notably, the performance of the prototype in outdoor weathering did not degrade during the testing period, despite temperature fluctuations from the warm summer sun to freezing temperatures, as well as copious amounts of snow resting on top of the prototype.

Key words: Encapsulation, Solar energy, Solar cells,

Diplomityö

Oppiaine: Materiaalitekniikka
Tekijä: Tommi Jokikyyny
Otsikko: Inert Liquid Encapsulation: A Novel Approach to Enhancing Lifetime, Thermal Stability, and Recyclability of Solar Cells
Ohjaajat: Prof. Kati Miettunen, TkT. Aapo Poskela
Sivumäärä: 43+11
Päivämäärä: 23.2.2026

Uusiutuvien energianlähteiden tarve kasvaa fossiilisten polttoaineiden riippuvuuden vähentyessä. Aurinkoenergialla on merkittävä rooli alalla, mutta tutkimuksen kohteena on ollut lähinnä hyötysuhteen kasvattaminen. Aurinkopaneelien eliniän kannalta olennainen komponentti, enkapsulointi, on jäänyt vähemmälle huomiolle.

Siten aurinkokennojen enkapsulointi on pysynyt samankaltaisena vuosikymmenet. Aurinkokenno laminoidaan ristisilloitetun polymeerin sisään. Tämä diplomityö esittelee uuden tavan enkapsuloida aurinkokennot inerttiin materiaaliin, joka voisi merkittävästi pidentää aurinkopaneelien elinikää samalla helpottaen niiden kierrätystä huomattavasti. Uusi enkapsulointitapa avaa tietä uusille modulaarisille kennoille, joissa enkapsulointimateriaali voidaan vaihtaa, keventäen kennojen negatiivisia ympäristövaikutuksia. Tässä työssä keskitytään yhteen potentiaaliseen materiaaliin, samalla ehdottaen muita korvaavia materiaaleja sopivilla ominaisuuksilla. Työhön valikoitunut materiaali on dimetyylipolysiloksaani.

Useita prototyyppejä valmistettiin sekä kunkin kyvykkyys testattiin joko karuissa ulko-olosuhteissa tai laboratorio-olosuhteissa.

Huomattavaa on, miten erityisesti ulkotestauksessa olleen prototyypin toiminta ei heikentynyt suurista lämpötilanvaihteluista huolimatta. Hetkittäin kenno oli suorassa auringonvalossa, ja muutaman viikon kuluttua 30 cm paksun lumikerroksen alla hyytävässä talvisäässä.

Avainsanat: Enkapsulointi, aurinkoenergia, aurinkopaneelit,

Table of contents

1 Introduction

Solar modules are typically relatively simple laminated modules of glass, polymer encapsulation, the active layer (silicon photovoltaic cells) and a surrounding structural frame to keep it all in one module. The polymer encapsulation used is usually ethylene-vinyl acetate (EVA). A common application where one might encounter EVA is hot melt glue as EVA is the most produced hot melt adhesive by volume [1]. This material is melted and crosslinked in a vacuum laminating process, and the produced solar module comes out as the aforementioned glass/plastic/silicon/plastic/glass (or other backing material) lamination. Considering the vast changes in operational temperature and the surrounding humidity that prevail throughout the lifetime of solar modules, the correct function of the encapsulation is vital. The best solution would completely isolate the cell from the outside environment. While EVA has some good qualities, it is not without its flaws, and failures do occur. Some modules fail due to cell manufacturing defects, while many fail due to the encapsulant itself. [2] The primary goal of my invention was not only to increase the lifespan but also to improve the recyclability of solar modules. Currently, recycling crystalline silicon photovoltaics is an energy- and resource-intensive process. Separation of the module components requires significant heat, and/or chemicals; high-temperature thermal processing is used to remove the EVA film, sometimes followed by chemical processing to strip the remaining materials. [3] [4] To eliminate these energy intensive, environmentally-unfriendly processes, this invention moves away from traditional encapsulation in favor of new liquid encapsulation materials, hereafter referred to as inert liquid encapsulation (ILE). By utilizing ILE, the need for thermal processing and harsh chemicals can be completely avoided. When using ILE, each of these energy and resource intense processes can be avoided.

The objective of this thesis is to prove that using ILE has several advantages over current solutions and is especially beneficial regarding recycling. This is achieved through material and design optimization. Two different prototypes were designed with differing design considerations. Because the module utilizes a liquid encapsulant, the initial prototype had an emphasis on the quality of the hermetic seal as a proof of concept. The second prototype had more realistic construction with both the ease of manufacturing and recycling, and long lifetime taken into consideration. Each of the hypothesized advancements were tested using applicable experimental setups. The results of these experiments were further reinforced by an outdoor aging experiment. No noticeable performance reduction was seen after the outdoor aging

experiment. The thermal performance of the chosen ILE material was tested using thermal imaging. Together these results suggest that ILE can be seen as a viable encapsulation method for some solar cell types.

2 State of the Art

The most frequently used material for solar cell encapsulation is EVA. In addition to EVA, other materials less commonly utilized include thermoplastic polyurethanes, polyvinyl butyral (PVB), different ionomers, resins, and silicones. Reasons for the success of EVA in encapsulation include cost, reliability and availability. EVA has been used for decades. Other less common polymers exist, but the main limiting factors are high costs and availability. As most of the encapsulation materials are polymers, additives, such as stabilizers and plasticizers are present. These materials are a known weak point as the necessary implementation of these materials introduces decomposition products that can negatively affect the cell performance and lifetime. Plasticizers are used to improve the mechanical properties of polymers, for example increasing the flexibility of encapsulation. Similarly, the exposure to ultraviolet (UV) radiation necessitates the use of UV stabilizers. As UV radiation has the energy to sever covalent bonds in the materials, this causes degradation. For solar modules, the UV radiation might be partly reflected on the modules' surface using UV reflective materials. However, commonly encapsulants might contain another line of defense for ultraviolet radiation, UV stabilizers. These materials absorb UV radiation and prevent or slow down degradation or react with the broken bonds in order to prevent them from participating in further degradative processes. [5]

2.1 Ethylene Vinyl Acetate (EVA)

Most common photovoltaic modules use EVA as the encapsulant. EVA is the only mainstream encapsulant with a proven track record as EVA has been used as encapsulant for many decades. EVA is known to have great optical properties and reasonable durability. While EVA is a popular choice, it does not come without limitations. Main problems are regarding UV degradation, moisture ingress and delamination. One particularly problematic aspect of EVA is the production of acetic acid catalyzed by water and/or UV exposure. For extreme conditions, such as space or arctic applications, EVA has problems with relatively high glass transition temperatures. [6]

2.2 Poly Vinyl Butyral (PVB)

The main difference when compared to EVA, PVB is a thermoplastic, whereas EVA is a thermosetting polymer. In practice, this means that once EVA is heated and cured, it forms irreversible bonds and cannot be melted again without destroying the material. PVB simply

softens as a thermoplastic when heated, allowing easier recycling process. PVB has excellent optical properties for photovoltaics. PVB has good mechanical strength and high adhesion strength, hence its common use as a safety glass lamination adhesive. PVB has a high hydrolysis tendency, which causes problems regarding the longevity of the polymer. [7]

2.3 Thermoplastic Polyurethane (TPU)

Thermoplastic polyurethane is rarely seen in silicon solar modules but is still a reasonable choice. TPU has comparable optical performance to EVA, but can be used without crosslinkers, and therefore has better UV stability. The use of TPU however, might come with problems regarding creep (slow deformation of the materials under continuous stress) and delamination (separation of the module components). [2] TPU has great transparency especially at the useful visible and near-infrared wavelengths, and a beneficial UV-cutoff zone, limiting the silicon solar cell's exposure to useless wavelengths. [8]

2.4 Thermoplastic Polyolefin (TPO)

Thermoplastic polyolefins are newer materials which possess better degradation properties regarding optical and thermal performance. According to one study, TPO has a nine times slower discoloration rate when compared to EVA. TPO has good UV resistance, but high water permeability, even when compared to EVA. [9]

2.5 Polyolefin Elastomers (POE)

These materials are polyethylene-based elastomers (polymers that have elastic, rubber-like properties). Like TPOs, POEs show good optical and UV resistive properties, but have problems regarding adhesion. This leads to the need to use adhesion promoters, which might cause degradation problems. [9]

2.6 Silicone

Silicone, or siloxanes, have great performance, especially in extreme conditions. Silicone encapsulants have notably been used in space applications for a long time. And some signs of interest in the commercial field have risen. Main drawbacks of silicones are the demanding processing conditions; they require precise mixing and long curing times. Furthermore, the recycling of cured silicone is harder as it cannot simply be melted and reused as thermoplastic polymers, but requires more advanced depolymerization processing. [10]

3 Material Selection and Characterization

Solar cell inert liquid encapsulation materials are crucial for the proper functioning of solar cells. The encapsulation protects the module while preferably affecting the optical properties of the cells as little as possible. The effects of the encapsulation materials on the electric performance of the cell should also be as low as possible.

3.1 Criteria

The following desired qualities are important for the inert liquid encapsulation material selection.

3.1.1 Transmission

For maximizing the performance of the solar cell, minimizing the effects on light transmission is advisable. Materials should be chosen with high transmittance at the wavelengths used. For silicon solar cells, the useful wavelengths are between 300 nm and 1100 nm. [11]

3.1.2 Refractive index

To create a smooth optical transition, the refractive index of the encapsulant should land between the refractive indices of the top surface material and the surface of the solar cell. This minimizes the losses occurring at the boundaries. Usually, commercial cells have anti-reflective coating on the surface of the silicon wafer. The refractive index of anti-reflective coatings is usually in the neighborhood of 1.9 to 2.1 for silicon cells. Considering the refractive index of glass is around 1.5 and if the refractive index of the cell is 1.9, a refractive index of 1.7 would technically be the best for minimizing the reflection losses in both interfaces. The best refractive index can be calculated by geometric mean, which in this case would be 1.69 [12]. While the differences in efficiency will be minimal between the different compositions of encapsulants, even small differences matter in the context of solar cell efficiency, where incremental gains lead to significant cumulative impact.

Such refractive indices are rare in liquids, though a few exceptions do exist. Achieving higher refractive indices requires an increased amount of interaction between the light and the material. Therefore, solid materials usually exhibit higher refractive indices than liquids. 1.4 to 1.59 are plausible refractive indices for silicon oils. The refractive index of silicon oils depends on the viscosity and the overall structure of the oil. Some silicone oils, such as phenylmethyl

polysiloxane have a promising refractive index of 1.515 [13]. Even more promising refractive index can be found in 1,1,3,5,5-Pentaphenyl-1,3,5-trimethylsiloxane, with refractive index of 1.555~1.588 [14].

3.1.3 Weather Resistance

Lifetime expectations for current solar modules hover around 25 or so years [15]. To achieve these expectations, the weather resistance of the encapsulation is crucial. For liquid encapsulation the weather resistance works differently than with solid or semisolid encapsulants. If water ingress occurs, a difference between densities would be beneficial. With lower density liquids, such as dimethylpolysiloxane, the water would sink to the bottom of the module and could be drained away. Vice versa, for higher density liquids, water would float to the top and could be purged away. How significant a problem the water ingress can be, remains to be seen. The highest focus should be on the structure of the module itself, the gasket between the top and bottom surfaces is the most important part for weather sealing.

3.1.4 Chemical Resistance

Good chemical resistance is a valued property, for both the outside elements, such as air pollutants and the inner chemical processes that might occur due to the exposure to sunlight. Reactivity should be as low as possible, as the encapsulant should not affect the structure of the cells' surface, as this might lead to premature degradation. [15]

3.1.5 Mechanical Properties

The mechanical properties are specified for the common photovoltaic modules, where the encapsulant acts as a supporting material for the complete module. The mechanical properties include the reactions to temperature changes, moisture and outside loads. Of the latter, the dampening of vibrations, or other external forces can be considered a factor of mechanical perspective. The mechanical properties of ILE are promising, as the material acts as a protective oil around the vulnerable part of the module. It is important, however, to note that the encapsulant will not participate in the mechanical stability of the module, which increases the structural rigidity demand for the surfaces and the frame of the module.

3.1.6 Glass Transition Temperature

The glass transition temperature (T_g) of encapsulation is an important factor. Glass transition temperature describes the temperature where the material undergoes a change from amorphous solid polymer into a more “flexible” state. [5] For EVA, this temperature is usually under 30°C. Materials with higher glass transition temperature are not suitable for solar cell encapsulation, as they become too brittle at lower environmental temperatures. Glass transition temperature is hence an especially important factor for solar modules intended for use in colder climates. Too high glass transition temperature could pose problems for the shock absorption and vibration reduction, as well as cause adhesion issues, as the adhesion usually depends on the material being in flexible state [6]. The glass transition temperature of the chosen ILE material lies well below -120°C, far beneath the thermal conditions expected in normal operational environments [16].

3.1.7 Adhesion

For “glue type” encapsulation, the adhesion strength is vital for proper lamination. If delamination occurs, it is usually non-reversible. Proper adhesion increases the structural properties of the module. [17] With ILE, adhesion is not a factor as the module in itself acts as the supporting structure for the system.

3.1.8 Electrical Properties

Encapsulants are preferred to exhibit high dielectric strength, resistivity, and overall electrical insulation properties, to prevent adverse effects on the electrical performance of the photovoltaic cells. With ILE the electrical conductivity should be as low as possible. The ILE material used, dimethylpolysiloxane, has excellent volume resistivity and acts as an insulator. According to the measurements described in [18], liquid silicones have a volume resistivity over 10^{13} Ω·m. EVA, has similar values, but unlike dimethylpolysiloxane, a significant drop does occur at higher temperatures [19]. The dielectric constant, which describes the material’s ability of storing electrical energy is low for dimethylpolysiloxane and silicones in general. Dimethylpolysiloxane possesses a dielectric constant of around 2.18 [20]. EVA has a dielectric constant of 2.5 to 3 [21]. It is beneficial to have as low dielectric constant as possible for encapsulants as this reduces electrical interference and the risk for potential-induced degradation (PID); a long-term power degradation process where high voltages between the parts of the module create current leakage.[22].

3.1.9 Easy Processability

Lamination of current photovoltaic modules is an error prone area of module manufacturing. Manufacturing defects such as delamination and air bubbles pose risk for the longevity of the module as well as decreasing performance. Delamination can be caused by poor quality materials, or suboptimal manufacturing conditions. Bubbling refers to small air bubbles trapped in the encapsulation during lamination stage. These can be caused by vacuum problems or other manufacturing errors. [17], [23] With ILE, neither of these are a problem as delamination of fluid is impossible, and bubbles simply rise to the surface of the liquid, away from the active layer. Comparing common photovoltaic module production, where moisture content of the modules is a noticeable problem, the water ingress during production of ILE modules can be mitigated by purging the completed module with dry gas and replacing the gas with the encapsulation liquid.

3.2 Distinctive Characteristics of ILE

3.2.1 Heat Management and Hot Spots

Due to the liquid nature of ILE, the encapsulation has constant contact with the photovoltaic cell. This combined with the good thermal properties of the chosen ILE, enables great thermal management of the cell. ILE acts as “water cooling” and with reasonable viscosity it transfers heat by thermal conduction enhanced by convection. In theory notable improvement can occur when “hot spots” are present. The current encapsulation methods trap the heat between the layers and act more as a static conduction-based thermal insulation layer. ILE alleviates this problem by facilitating dynamic natural convection and staying in constant contact with the more thermally stressed area. [24]

3.2.2 Recycling

Due to the inherent difference of encapsulation methods, liquid encapsulation is considerably easier to remove when recycling the module. The current method for commercial photovoltaic module recycling usually consists of shredding the module into fine pieces, and/or chemically treating the wanted components. [25] With ILE one can simply drain the liquid from the module and continue disassembly as needed. This can be hypothesized to be the most influential benefit

of the inert liquid encapsulation, considering the growth in photovoltaic module production, and therefore the increased need of end-of-life recycling [26].

3.2.3 Regeneration

One possibility that ILE introduces, is the potential to “regenerate” the encapsulation in situ. The encapsulation can be either changed or purified without disassembly of the module. The purification can even happen automatically. According to the current understanding of the aging mechanism, the ILE can be simply filtered through a fine filter and introduced back into the module. This method could be used to increase the lifetime of the modules at the site of use without the need for transportation for maintenance or even disconnecting the panel from the grid. Constant flow cooling- and purification loop is one of the possibilities. The encapsulant could flow with adjustable flowrate from the top of the cell down into the bottom, through a cooling system (radiator etc.) and into a filter.

3.2.4 Off Gassing

Common encapsulation materials have additives and residues from the production phase. These materials can create vapors or volatile substances in a phenomenon called off gassing catalyzed by solar radiation, heat, and moisture. Off-gassing poses challenges for encapsulation materials as it can affect the performance of the module. [23], [27] ILE material can be chosen to minimize the off-gassing potential. Production of volatile substances, and or vapor from the chosen ILE material in this thesis is not expected, as dimethylpolysiloxane does not suffer from off-gassing, due to absence of acetate groups and low vapor pressure [20]. Therefore, the probability of off-gassing occurring and affecting performance is low.

3.2.5 Reduced Mechanical Stress

During environmental changes occurring under normal conditions, normal solid or semi-solid (rubbery) encapsulation materials transfer mechanical stress into the solar cell wafers and strings. This does not occur with liquid encapsulation, and therefore stresses related to encapsulation are minimized. Mechanical stress also occurs due to outside forces, such as snow

loads during winter. “Normal” encapsulation materials transfer these loads into the active materials. As with thermal induced stresses, these loads are also reduced by the intrinsic qualities of liquid encapsulation. Due to the uniform distribution of forces in a liquid, the effect of pinpoint loads, such as those that might occur during transportation, are not transferred into vulnerable active materials.

3.3 Properties of Dimethylpolysiloxane

The ILE material selected for this research is dimethylpolysiloxane (dimethicone) shown in Figure 1**.** This material has good optical and electrical properties while being extremely unreactive: The transmittance for light in the usable range of silicon photovoltaics is high, and absorption is low.

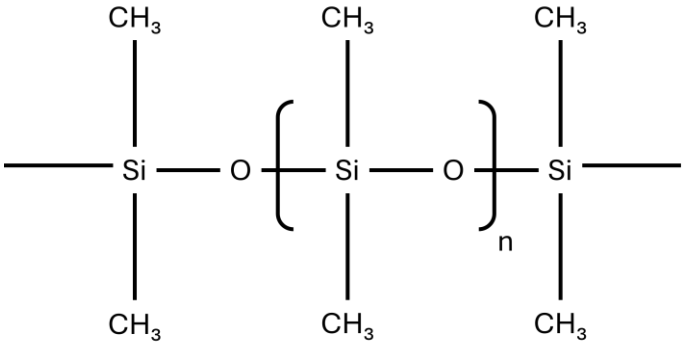

Figure 1. Average Dimethylpolysiloxane structure (Jokikyyny)

Dimethylpolysiloxane has a refractive index that is reasonable, though it can be modified in a narrow range by altering the molecular side groups [28]. Electrical performance is one of the main benefits of this material as dimethylpolysiloxane can be considered both electrically and chemically non-reactive. The physical properties of dimethylpolysiloxane can be chemically modified. For example, maximizing the effectiveness of thermal convection, the viscosity of fluid can be altered by controlling the molecular weight of the fluid [29]. The thermal performance is also an extremely good fit for PV encapsulation. Dimethylpolysiloxane has a low freezing point of -55 °C, and high boiling point of over 140 °C at 0.003 hPa. Availability-wise dimethylpolysiloxane is one of the most used organic silicon-based materials. It is widely used in the cosmetic industry, and scientific applications. Even some foods have dimethicone as anti-foaming agent. [30]

4 Methodology

This chapter outlines the methodology used. It describes the design of the experiments, prototype and reference cell design from start to finish, and the data collection methods and research approach used.

4.1 Experimental Design

Within the scope of this thesis the experimental design was simple and efficient. The basic design was to produce a working prototype and test its viability in outdoor aging setup. Each of the proposed benefits of ILE were to be tested individually. Main emphasis was set on the outdoor test in Finnish conditions.

Two different types of prototypes were constructed for the experimental section. One full M6-sized (166 mm x 166mm) cell prototype, with emphasis on sealing reliability and optical performance. Several glass-based test samples were additionally made for the experiments that require disassembly of the modules. These samples used miniature monocrystalline silicon cells.

Outdoor aging setup: Initial prototype, Prototype A, was mounted outside on the roof of a University of Turku building in a frame at 45° pointing at 115° degrees Southeast as shown in Figure 2. The prototype was left stationary without load and removed a total of five times for cyclic voltammetry (CV) measurements. A PalmSens 4 potentiostat was used for the CV measurements. The settings for the measurements are visible at Table 1.

Initial E (V)	-0.2
Scan Limit 1 (V)	0.55
Scan Limit 2 (V)	-0.2
Final E (V)	-0.2
Scan Rate (mV/S)	50
Step Size (mV)	10
Cycles (#)	1
Sample Area (cm^2)	1
I/E Range Mode	Fixed
Sampling Mode	Noise Reject
Max Current (mA)	150

Equilibration Time (s)	2
PF Corr. (ohm)	50

Table 1. PalmSens Settings

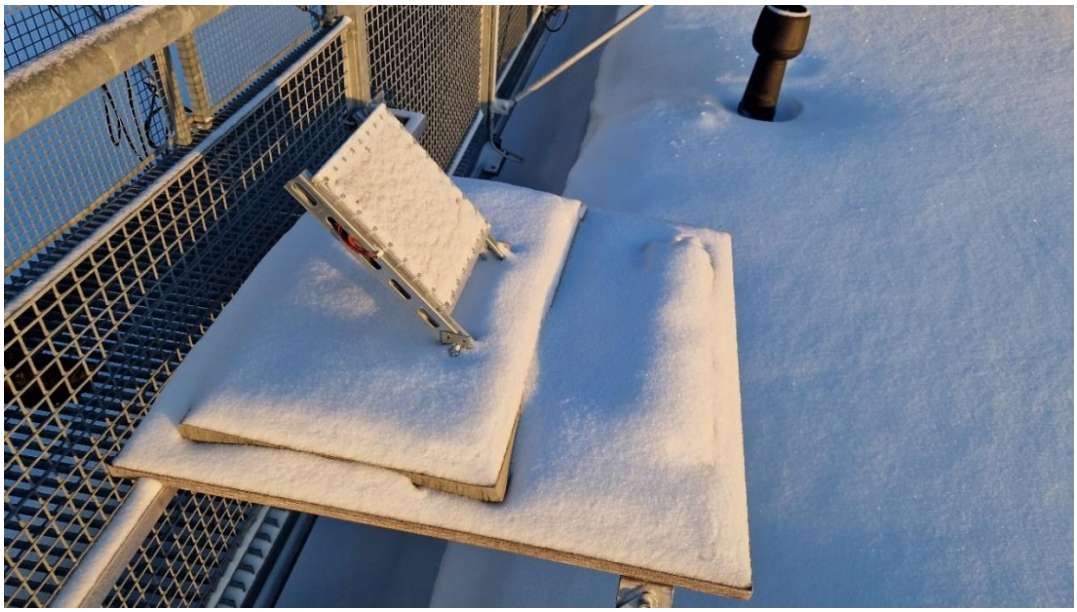

Figure 2.The outdoor aging setup. This prototype was subjected to outside elements for nine months.

The weather data from the outdoor aging experiment period is shown in Figure 3. Rainfall was abundant during the fall and maximum snow depth was achieved mid-February at 28.3 cm. The coldest temperature from the measurement period was -23°C. The weather data is from 5.6 km away from the experimental site, Artukainen Turku. Average daily temperature, as well as rainfall and snow depth are useful measures of the average conditions at the measurement site. Source for the data was the Finnish Meteorological Institute databank [31].

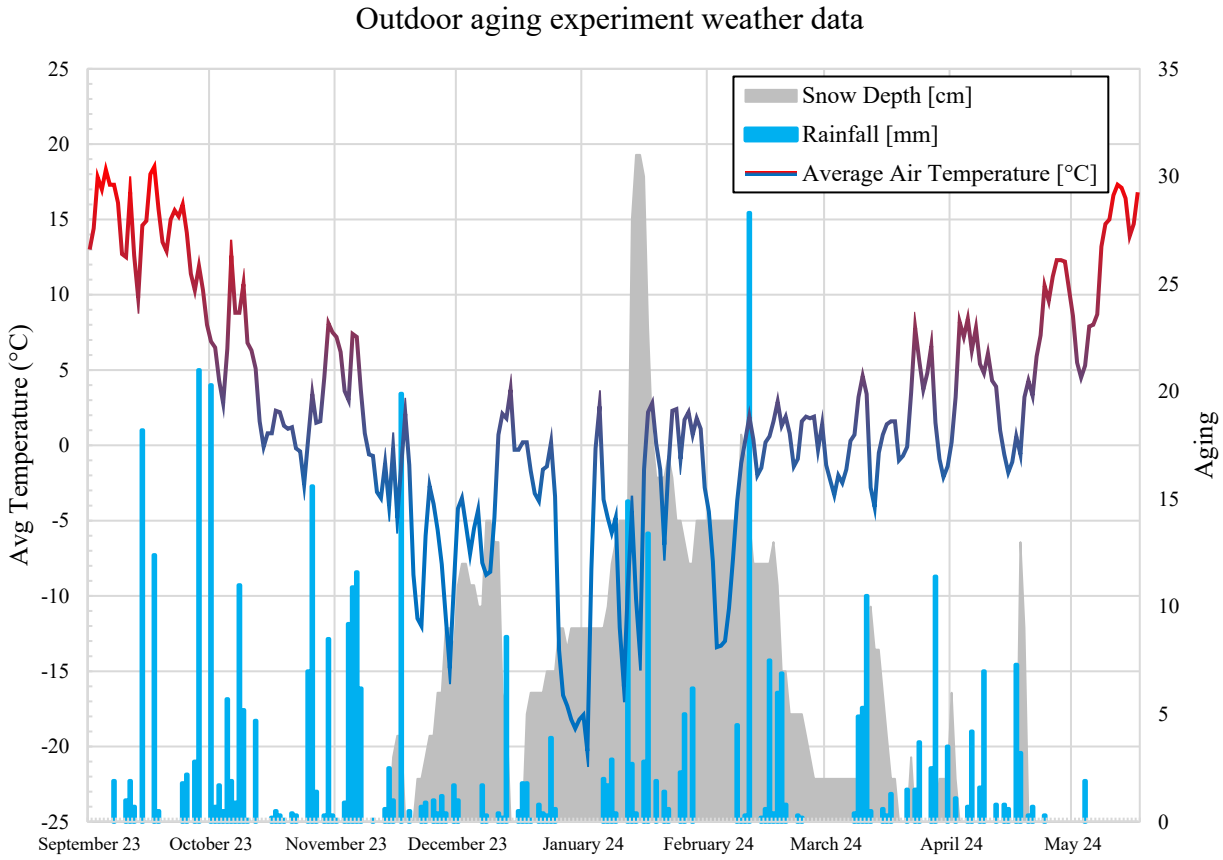

Figure 3. Weather data through experimental period. Source (FMI)

Thermal performance measurement: The proposed effect of ILE is improved thermal performance. Preliminary testing before the prototype samples were ready was conducted using finite element method (FEM) modeling in COMSOL 6.2, without the computational fluid dynamics (CFD) module. This limitation reduced the realism of the simulations as convective currents could not be accurately modeled. Due to convection, ILE can more efficiently transfer heat from areas of higher temperature and thus increase the overall performance. The effect of convection on heat transfer was studied using the following approach: an electrical current was applied to the encapsulated photovoltaic cell. The produced heat will then conduct to the outside surfaces and dissipate into the surrounding air. The heat transfer of EVA and the used ILE material are quite similar (EVA 0.21 – 0.24 W/m·K and Polydimethylsiloxane 0.15 – 0.16 W/m·K)[32], [33]. But the effect of conduction must be considered. This experiment thus measures the proposed increased thermal performance of liquid encapsulation. Several research methods were considered, with an experimental setup based on thermal imaging deemed most likely to yield relevant results. Thermistor-based measuring setup would not produce reliable

results as the temperature gradient on top of the glass might suffer from undesired effects. With thermal imaging a comparative study can be performed, where the performance can be visually compared, in addition to the quantitative approach. Problems associated with thermal imaging-based method include the possible differences between emissivity of the surfaces and the usual problems regarding thermal imaging of glass surfaces (reflectivity of IR light). The measurement setup can be seen in Figure 4.

Figure 4. Simple measurement setup for the thermal performance

Visual disassembly comparison: For presenting the easier disassembly, hence easier recyclability – Photographs of the system, and the steps of disassembly and result, ILE vs EVA were taken. The photographs are useful for qualitative analysis of the disassembly process. Quantitatively measuring the time elapsed during the disassembly and/or recycling process can act as an indicative value for the processes. Photographing is also beneficial as the images can easily visualize the destructiveness of the disassembly methods, and therefore how the disassembly affects the upcoming stages of the recycling processes.

4.2 Prototype Design

Two different types of prototypes were developed for the differing experimental setups. The first prototype was used as proof of concept, and later for the outdoor experiment. The latter prototype was developed at the end of the outdoor experiment period, with emphasis on creating a realistic solution with commonly used materials and easy recyclability.

4.2.1 Initial Prototype

For the proof of concept, a robust design was favorable. The prototype should be able to withstand harsh Finnish weather conditions with the included temperature fluctuations without compromising the integrity and reliability of the encapsulation. For achieving proper results, the maintaining of perfect sealing from outdoor elements was crucial. Therefore, the design was developed with absolute emphasis on the edge seals and waterproofing. Cost effectiveness, the assembly requirements and other more economical views were not incorporated in this prototype. The initial prototype consists of two polymethyl methacrylate (PMMA) sheets. The upper sheet has through holes for M3 cap head screw and lower has matching threaded holes. A cut-to-shape food-grade nitrile rubber (NBR) gasket is fitted between these layers to provide sealing, expansion resistance, and easy disassembly. A fill port was also incorporated into the upper surface by a threaded M3 hole with a separate O-ring gasket, together with a stainless-steel round head flanged hex screw. Figure 5 illustrates the basic structure of the first prototype. Figure 6 is a top view of the screw based single cell prototype, “Prototype A” containing section view A-A.

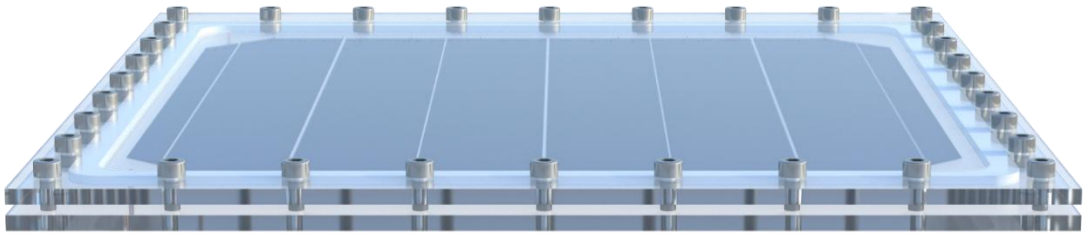

Figure 5. Computer generated illustration of the initial prototype cell.

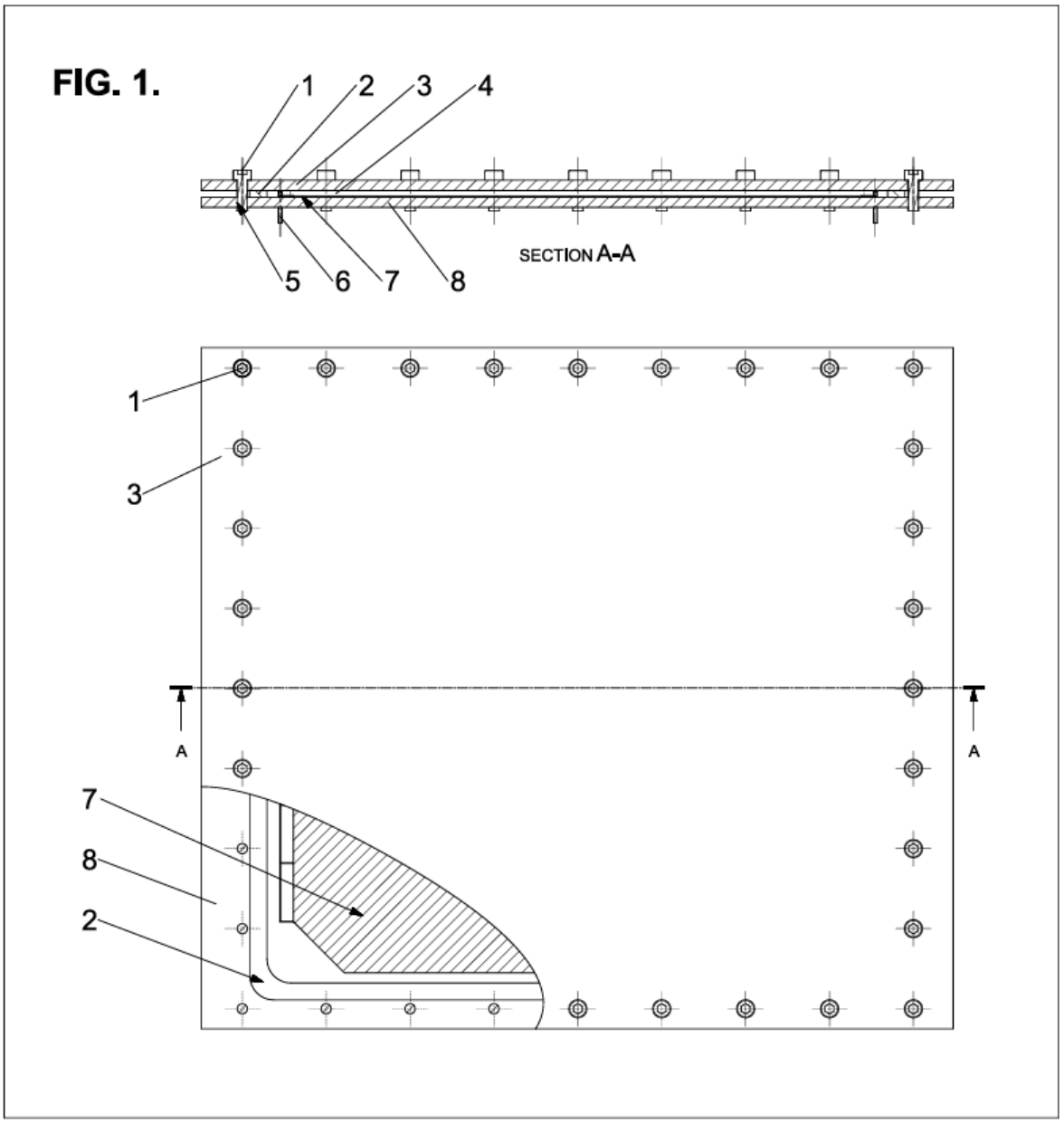

Figure 6. A top view of the screw based single cell prototype, “Prototype A” containing section view A-A pos. 1 – Cap head screw, pos. 2 – Gasket, pos. 3 – Top surface, pos. 4 – Inert liquid, pos. 5 – Thread, pos. 6 – Electrical contact, pos. 7 – Photovoltaic cell, pos. 8 – Bottom surface

4.2.2 Refined Prototype

For the second prototype a more reasonable solution was required. This was to be built with materials able to withstand years of outdoor real-life use, while maintaining the encapsulation performance and the ease of recyclability. The second prototype design process started with the consideration of the weak points of Prototype A, as well as the current system design on commercial modules. The weak points were the unfavorable attributes related to the screw-

based construction of Prototype A, and the use of PMMA, instead of more suitable glass materials. From the commercial modules, the aluminum frame was deemed as important regarding the possibility of installing the modules on existing equipment. The aluminum frame also protects the module and can be easily recycled. The refined module can be seen in Figures 7 and 8.

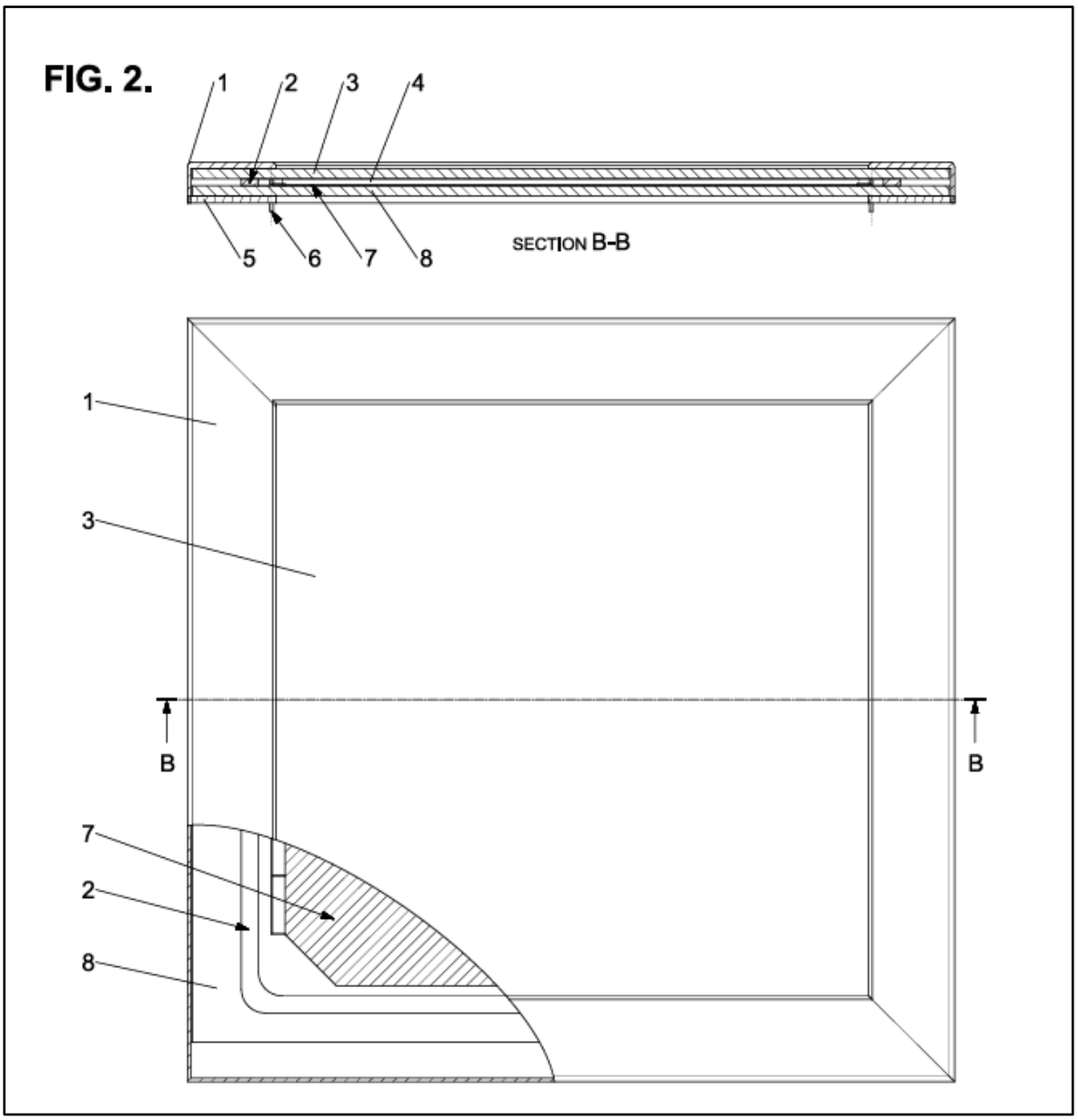

Figure 7. A top view of the crimp based single cell Prototype B containing section view B-B

pos. 1 – Top aluminum profile, pos. 2 – Gasket, pos. 3 – Top surface, pos. 4 – Inert liquid, pos. 5 – Lower crimped aluminum profile, pos. 6 – Electrical contact, pos. 7 – Photovoltaic cell, pos. 8 – Bottom surface

The proposed solution was not easily produced with facilities and tools available at the university, so a design with easier manufacturing process was developed. The basic module was to be independently assembled and only afterwards installed into the aluminum frame. Therefore, the frame would not be taking part in the sealing of the system. This also gave possibilities for changing the thickness of the components individually during the design process. A normal gasket as seen on Prototype A, was used and the whole construction was held together with simple spring steel clips. The clips produced the necessary pressure for the sealing of the gasket. The clips would also function as compensators for the expansion of the gasket, if it were to occur during the tests. Therefore, a small expansion gap was designed into the clips. The gap would also hold the assembled module centered in the surrounding aluminum frame. The aluminum frame was added to provide extra support and ease of handling. For easier and more accurate experimental measurements, this design uses $1/4^{th}$ sized cell with only one busbar. Using the smaller size, it also decreased the size of the completed modules, which helped with the experimental phase. The design of this easy-to-manufacture module can be seen in Figure 8. Prototype B was built according to the schematic shown in Figure 9.

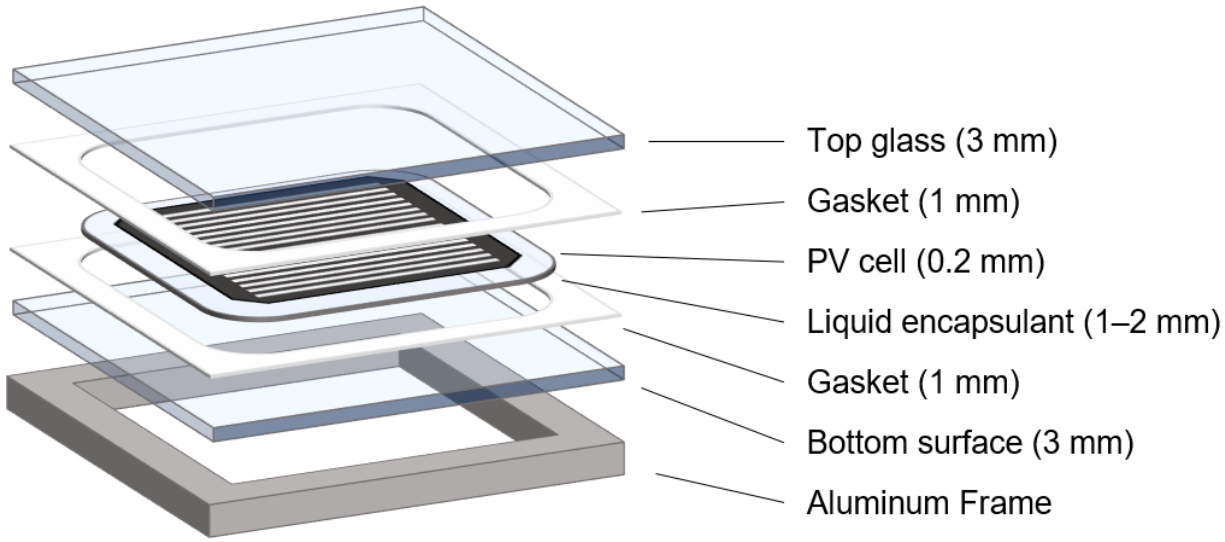

Figure 8. Deconstructed view of the refined ILE module

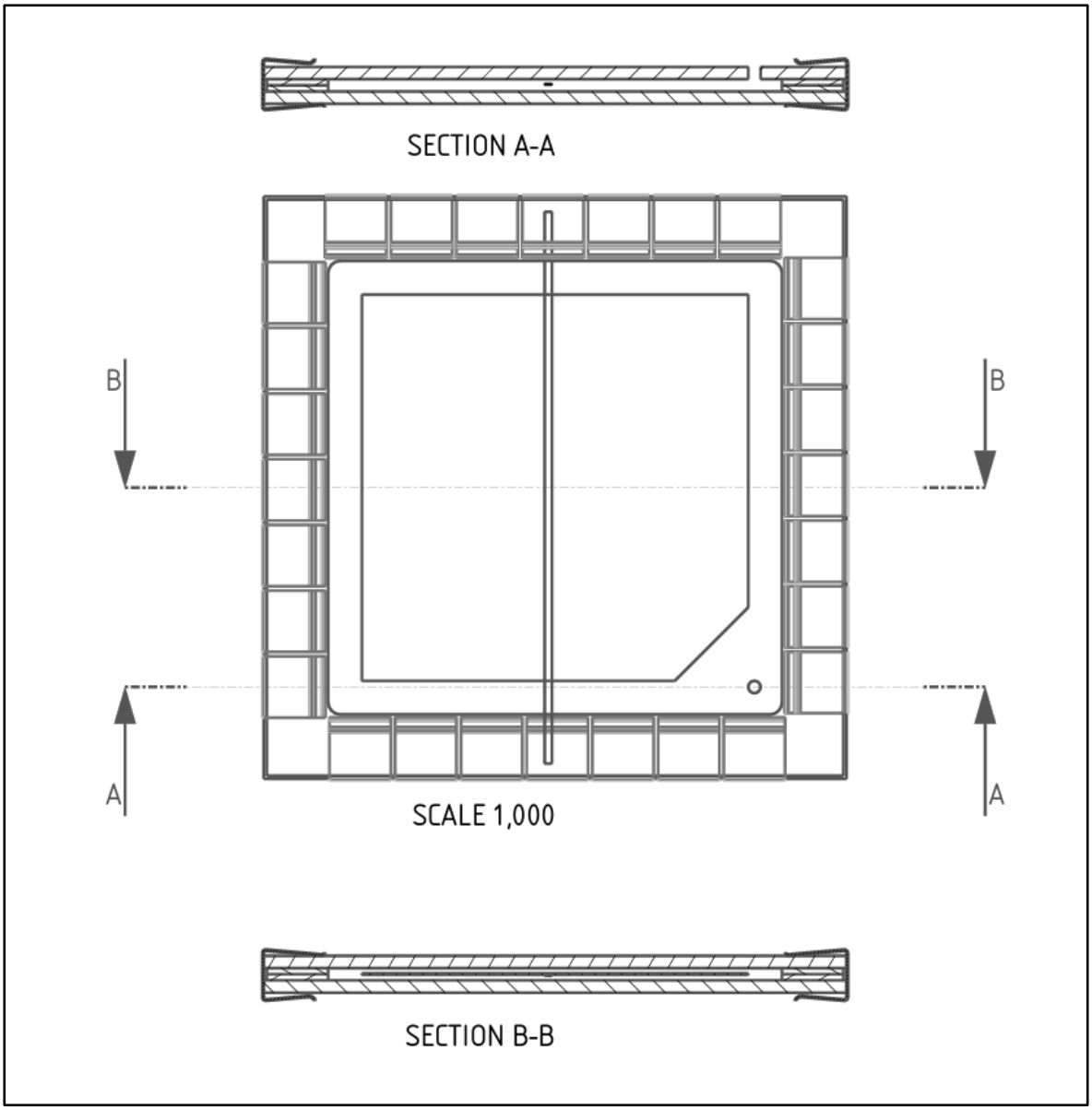

Figure 9. A top view of the steel spring version of Prototype B containing section views A-A and B-B. Section view A-A showcases the fill port while B-B shows the overall cutout view of the assembled module. This is the final version for the experimental setup.

4.2.3 Proposed Improved Design

During the design process of Prototype B, the prototype evolved into a better design with fewer parts. This design was, however, not built due to the time constraints and availability of manufacturing processes needed. This prototype was of similar construction of the first proposed aluminum frame-based system, Figure 7, but with even simpler construction. The basic idea was to use a shaped extruded gasket that holds the lower and upper materials together and provides environmental protection, sealing and expansion / vibration isolation for the components. The economic viability of this design was significantly higher than the former designs because of the reduced component count and significantly easier assembly process. The design can be seen below in Figure 10.

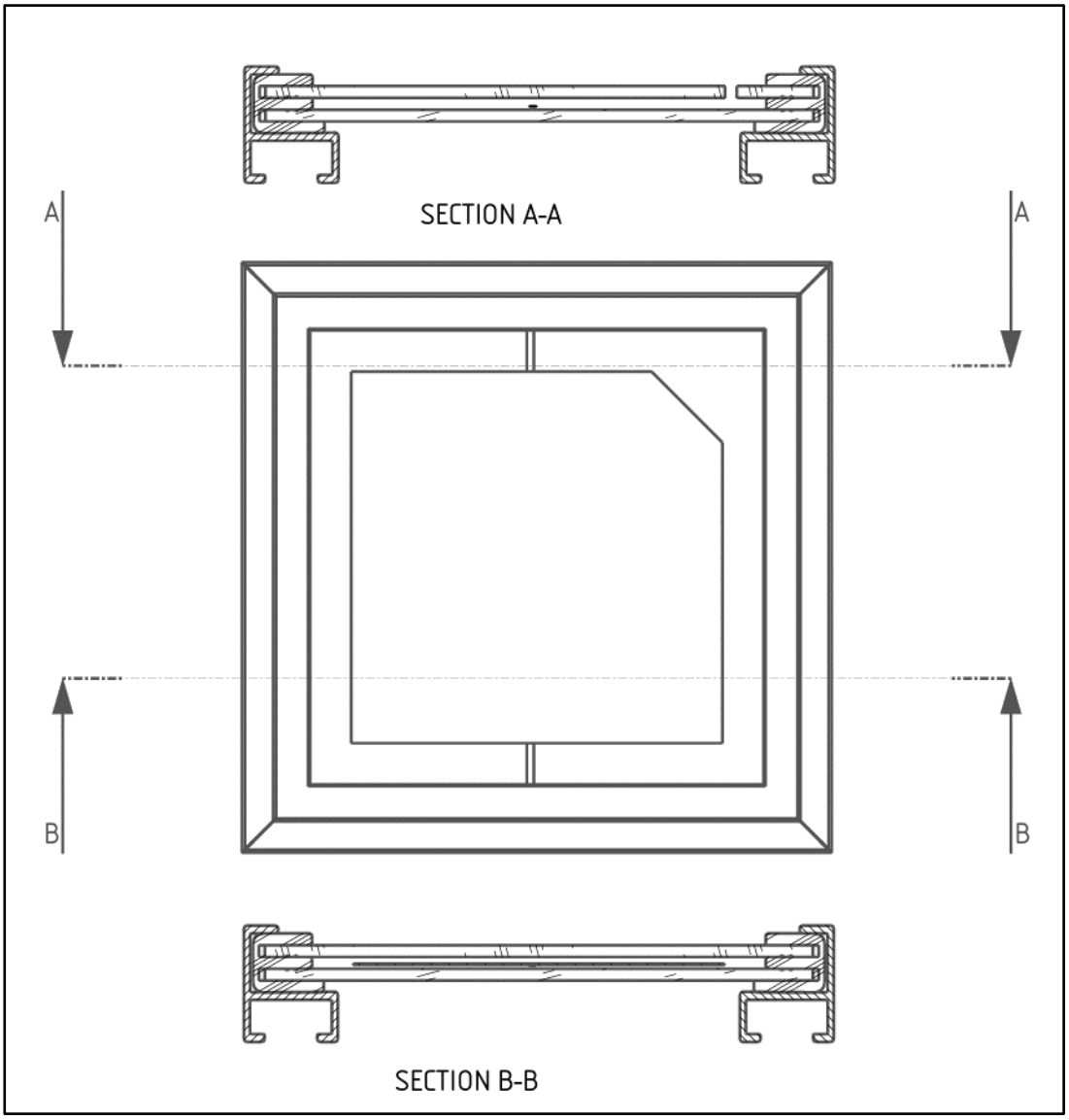

Figure 10. Top view of the proposed improved version containing section views A-A and B-B. Section view A-A showcases the fill port while B-B shows the overall cutout view of the assembled module.

4.3 Reference Cell Design

As most of the experiments are based on comparing the performance of ILE against currently dominating alternatives, a reference cell was needed. This was to be constructed in a manner similar to the commercial modules. For simplicity and comparability, glass was selected as the material for both superstrate and substrate. Since ILE can be used for bifacial solar modules, a glass back face (substrate) is also beneficial in this application. The glass used is just ordinary 3 mm soda-lime glass. High purity reduced iron content glass, usually used in optical applications, and solar modules, was deemed too expensive and unnecessary due to the comparative nature of the study. [34]

4.3.1 Construction

Commercial solar modules follow a simple design philosophy. Back sheet, encapsulant, cell, encapsulant and top sheet. For the reference cell, similar composition was needed. The reference cells consist of bottom glass as the substrate, bottom EVA film, PV cell, top EVA film and top glass. Differences from commercial modules are the use of normal soda-lime glass apart from low iron glass, and the use of glass as the substrate as this is usually replaced with lower cost, and weight, options such as polymers. The design of the reference cell is visible in Figure 11.

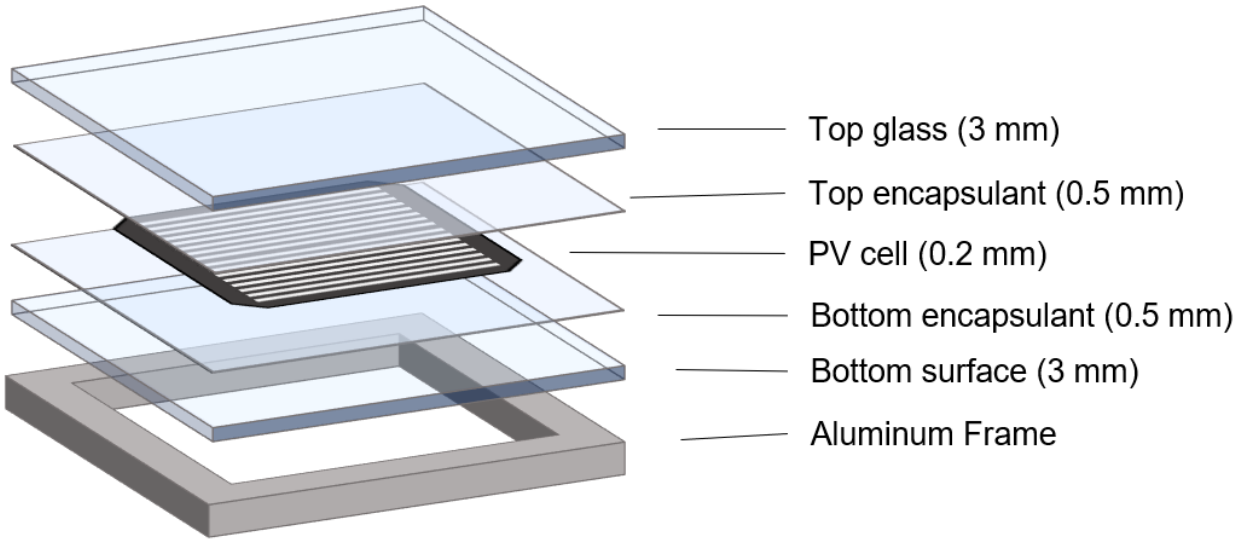

Figure 11. Deconstructed view of reference EVA cell

4.3.2 Assembly Process

The assembly of the reference cells was made in a similar manner to the commercial process. A commercial heated vacuum laminator P-Energy L150 was used for the lamination process. The modules were pre-assembled using EVA film cut from a freshly opened roll from dry storage container. The pre-assembled module was placed into the silicon vacuum pocket inside the laminator and the process was started. The recipe used was as shown in Table 1.

Phase	Time (s)	Temperature (°C)	Vacuum (mbar)
Prestart	60	20	1000
1	20	28	1000
2	300	50	0
3	180	50	0
4	720	135	1000
5	300	155	1000
6	1200	155	1000
7	660	50	1000
8	540	20	1000
9	0	20	1000

Table 2. EVA lamination recipe

After the cooldown period, the completed modules were removed from the laminator and placed into dark storage. The finished modules had visible air bubbles in the encapsulation, the cause of which was not clear. Usually, air bubbles occur during lamination if the EVA-film has excess moisture present. This was not the probable cause because two different batches of film were used during preliminary testing, one of which was from a new batch stored in a dry container with copious amounts of desiccant present. The relatively small surface area combined with a laminator designed for large-scale modules was deemed as the primary cause. The air bubbles were so miniscule that the probability of them affecting the function of the reference cells was deemed to be low. One reference cell with manual lamination process was however assembled for the purpose of testing the effect. This module was laminated successfully without visible air bubbles, using a simple laboratory oven with the same temperature recipe. Lamination pressure was provided by simple steel clips. This process did not include the use of a vacuum.

4.4 Data Collection

The Initial Prototype was left in outdoor conditions for nine months, during which it was removed and analyzed using cyclic voltammetry under simulated sunlight. The module was tested five times during the experimental period. The cell was covered with a black aluminum foil mask with precisely cut holes at two locations. One hole location was marked S1 and the other S2. Both of these locations were measured on each measurement occasion in an effort to decrease the measurement imperfections.

A thermal imaging video was the main source of data for the thermal performance analysis. The videos show both the overall temperature distribution via manually set limits and a temperature color gradient. Highest and lowest temperatures with their respective locations were constantly recorded using the camera inbuilt setting. Overall thermal performance can be studied both visually and quantitatively using the thermal gradient and numerical values provided.

4.5 Research Approach

The chosen research method consists of mostly experimental approaches with the chosen experimental setup. The experiment produces quantitative data that can be analyzed. However, due to the capabilities available, the aging experiment is not conducted in a controlled environment, but in real life environment, i.e., outside aging test.

The thermal conduction test was conducted in laboratory conditions with controlled parameters.

The recyclability of the module, being a more subjective opinion, was evaluated based on the time required, and the effort needed for the disassembly of the prototype module when compared to the sample module made with the commercial vacuum lamination process. The disassembly process was also photographed, in order to provide a more concrete view of the whole process.

5 Encapsulation Performance

5.1 Experimental Results – Outdoor Aging

On the 5th of September 2023, the outdoor experimental phase was initiated, using a full M6-sized cell prototype designated as Prototype A. On the 27th of September, following a three-week interval, the module was retrieved from the outdoor frame and cyclic voltammetry (CV) measurement was conducted under the simulated light of one sun. Subsequently, a third CV measurement was performed on the 7th of November. Following the third measurement, a fourth CV measurement took place on the 16th of January. No noticeable degradation in the cell performance was observed between the first and last measurements. When the unit was finally retrieved from the roof on 22nd of May, the last degradation CV measurement was done. Due to outside limitations, this measurement was done using a different potentiostat type, although better for this task – **Gamry 600+**. No visible degradation was noted when comparing the first measurement of September 5th to the last of May 22nd. The following graphs illustrate the graphical results and their associated numbers of importance. The graphs include both forward and reverse scans as there is little difference between them.

Figure 12 exhibits some quite peculiar data; it suggests an increase in cell performance. Both the fill factor and the efficiency have increased during the nine months of outdoor aging. This, however, is not likely the case, as these small differences are due to measurement errors and the use of two different measurement devices as explained earlier.

Considering the reliability limitations of the comparison between the initial and final measurements, where the measurement device was different, a more direct comparison can be made between the measurement from 5.9.2023 and 16.1.2024. shown in Figure 13. The same illogical increase in the short circuit current and efficiency can be seen. The fill factor is slightly lower, which is reasonable. One can only speculate the absolute reasons behind the irregularities, but the experimental setup was far from perfect as the main objective was to only prove the feasibility of the encapsulant type.

As a conclusion, no measurable degradation could be determined.

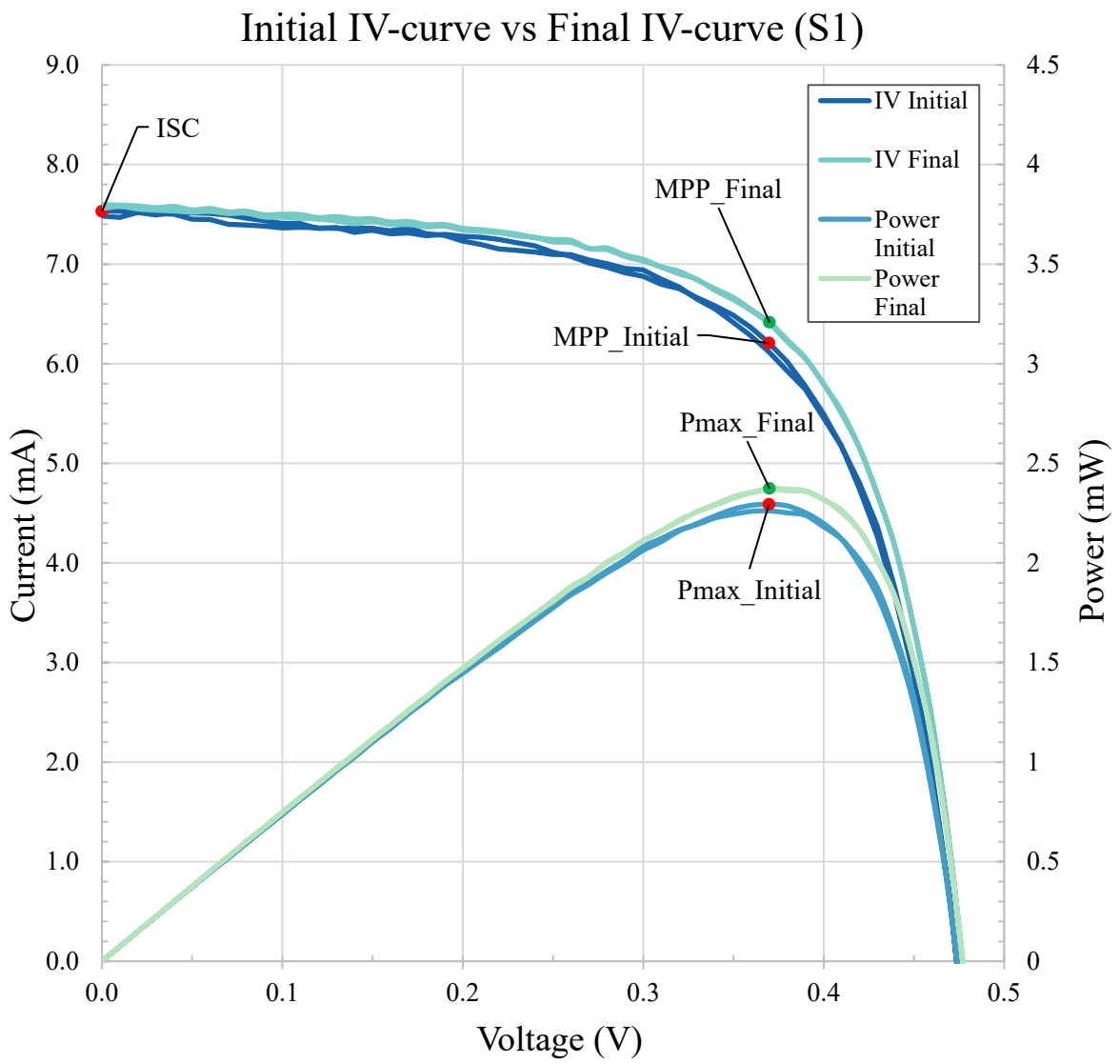

Figure 12. Comparison between the initial and the final measurement from sample point S1

Initial measurement 5.9.2023		
Area	0.13	**cm²**
Irradiance	1000	**W/m²**
P_{IN}	12.57	**mW**
I_{SC}	7.53	**mA**
V_{OC}	0.47	**V**
V_{MP}	0.37	**V**
I_{MP}	6.21	**mA**
J_{SC}	59.93	**mA/cm²**
FF	64.88	**%**
Efficiency	18.26	**%**

Final measurement 22.5.2024		
Area	0.13	**cm²**
Irradiance	1000	**W/m²**
P_{IN}	12.57	**mW**
I_{SC}	7.58	**mA**
V_{OC}	0.47	**V**
V_{MP}	0.37	**V**
I_{MP}	6.42	**mA**
J_{SC}	60.32	**mA/cm²**
FF	66.65	**%**
Efficiency	18.89	**%**

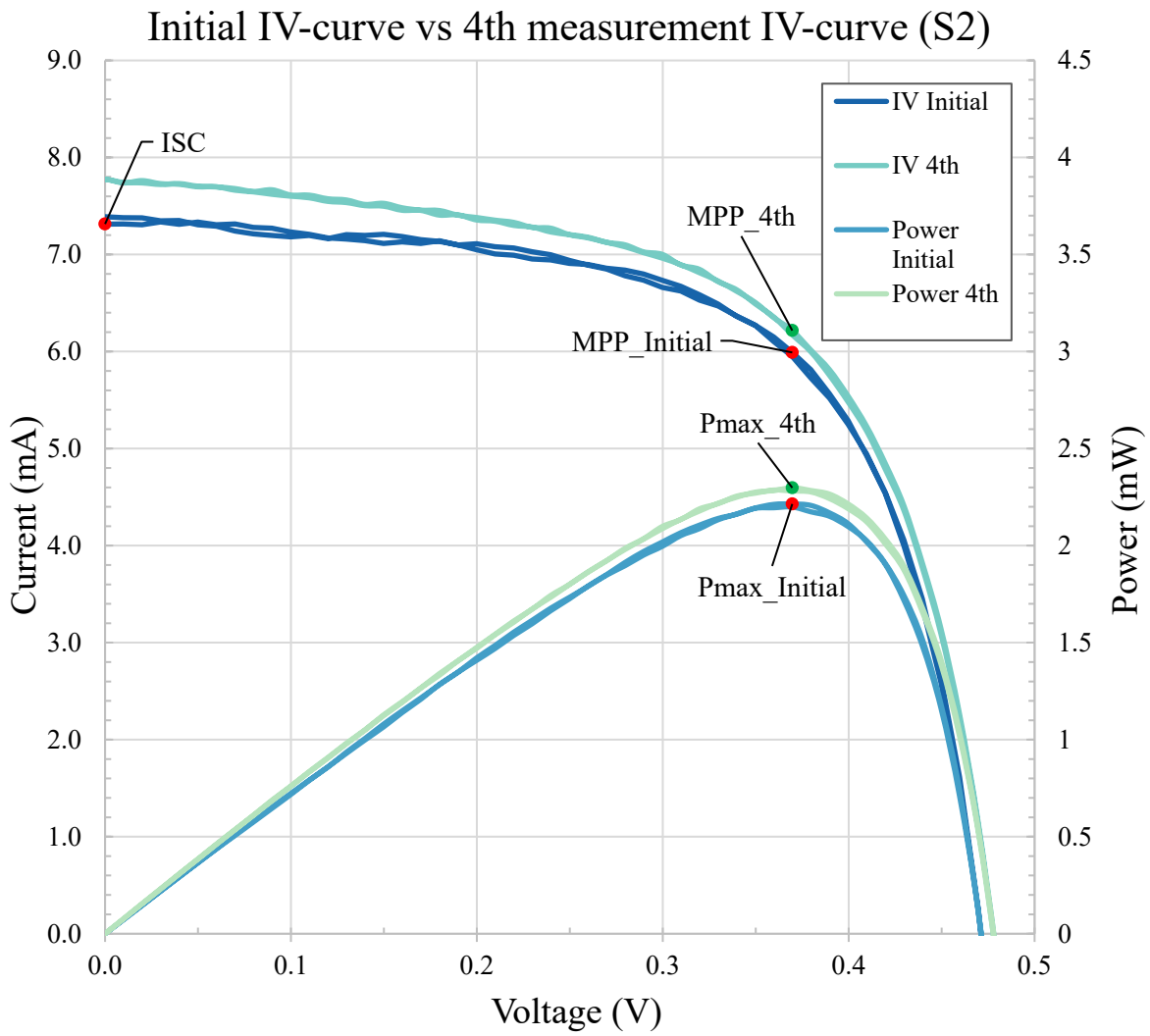

Figure 13. Comparison between the initial and the fourth measurement from sample point S2.

Initial measurement 5.9.2023		
Area	0.13	**cm²**
Irradiance	1000	**W/m²**
P_{IN}	12.57	**mW**
I_{SC}	7.31	**mA**
V_{OC}	0.47	**V**
V_{MP}	0.37	**V**
I_{MP}	5.99	**mA**
J_{SC}	58.21	**mA/cm²**
FF	64.46	**%**
Efficiency	17.62	**%**

4th measurement 16.1.2024		
Area	0.13	**cm²**
Irradiance	1000	**W/m²**
P_{IN}	12.57	**mW**
I_{SC}	7.74	**mA**
V_{OC}	0.47	**V**
V_{MP}	0.37	**V**
I_{MP}	6.22	**mA**
J_{SC}	61.62	**mA/cm²**
FF	63.20	**%**
Efficiency	18.29	**%**

5.2 Experimental Results – Thermal Performance

The effects of ILE were preliminarily studied using finite element method (FEM). The simulations were used for determining whether a full-scale experiment was necessary. FEM simulations were conducted using COMSOL 6.2 and the simulations were done for a few different experimental designs. The thermal performance of different encapsulations was modeled using both uniform and spot-based heat sources. Due to the need for advanced computational fluid dynamics, this research method was seen as questionable at best, as the modeling of fluid dynamics in such small volumes and spaces is considered challenging. Simple laminar flow modeling did not show improvement in the thermal performance, and so a real-life experimental setup was seen as the most viable option. Figures 14 and 15 display the simulated thermal performance of the reference cell, versus ILE cell. The simulation consisted of silicon wafer embedded in top and bottom layers of encapsulation material and glass surfaces. Both the reference and ILE simulations had the same thermal energy load on the wafer. The maximum temperatures were recorded and are visible in the middle of the illustrations. As mentioned, the analysis was inconclusive, as the liquid layer was modeled without computational fluid dynamics package. This eliminated the benefit of liquid heat transfer via convection within the liquid layer.

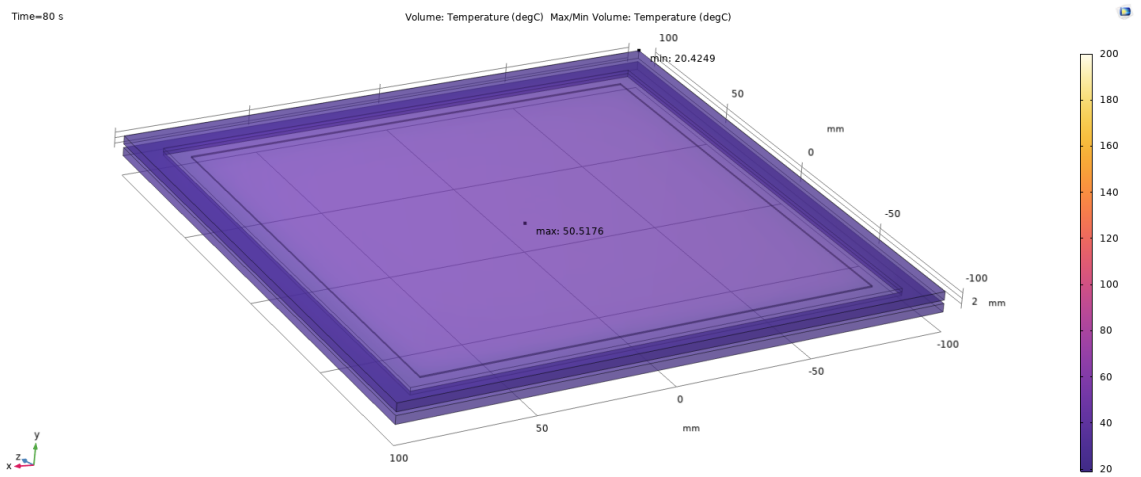

Figure 14. FEM analysis of reference EVA material

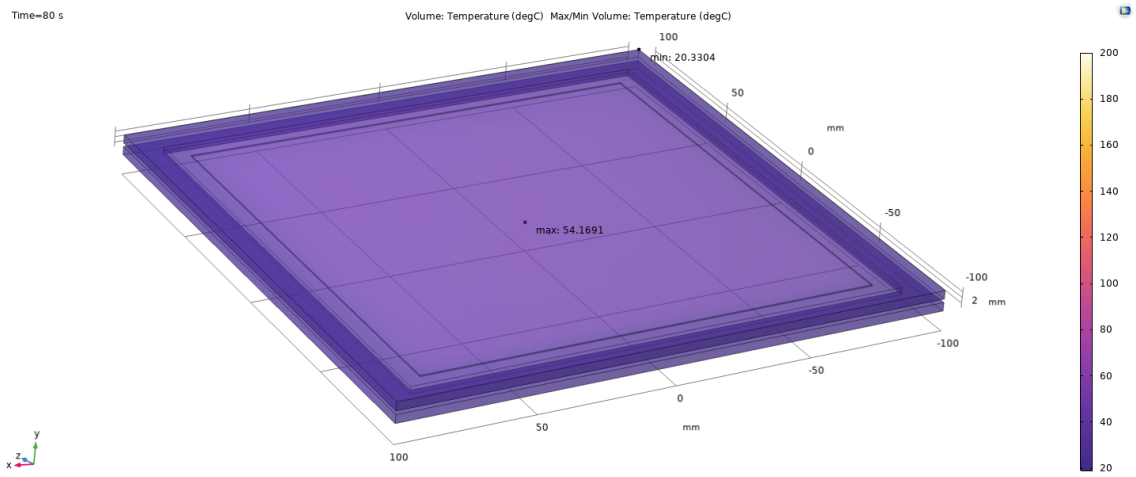

Figure 15. FEM analysis of ILE

As the simulations were inconclusive, an experimental setup consisting of a thermal camera and a laboratory power supply was set up. Here a fixed heat amount was given to both the reference cell, as a control, and the ILE cell. Due to the limitations of the power supply, the power input was set at 5.71 W. Each of the samples received a load of 5.71 W for 2 minutes, after which the load was disconnected, and the samples were left to cool for 10 minutes. The whole experiment was captured on thermal imaging video using a FLUKE TiS75+ thermal camera. The principle behind the experiment was to see how the temperature of the cell changes depending on the encapsulation material used. The thermal performance of the inert liquid encapsulation under semi-uniform heat load appears to match that of EVA, the reference material used.

The settings used for the thermal imaging camera were emissivity of 0.92, transmissivity of 100 % and a background temperature of 22 degrees C, as this was the temperature of the laboratory itself. The camera was set on a stand and recorded each sample uninterrupted. The following Figures 16–22 show the results of this experiment.

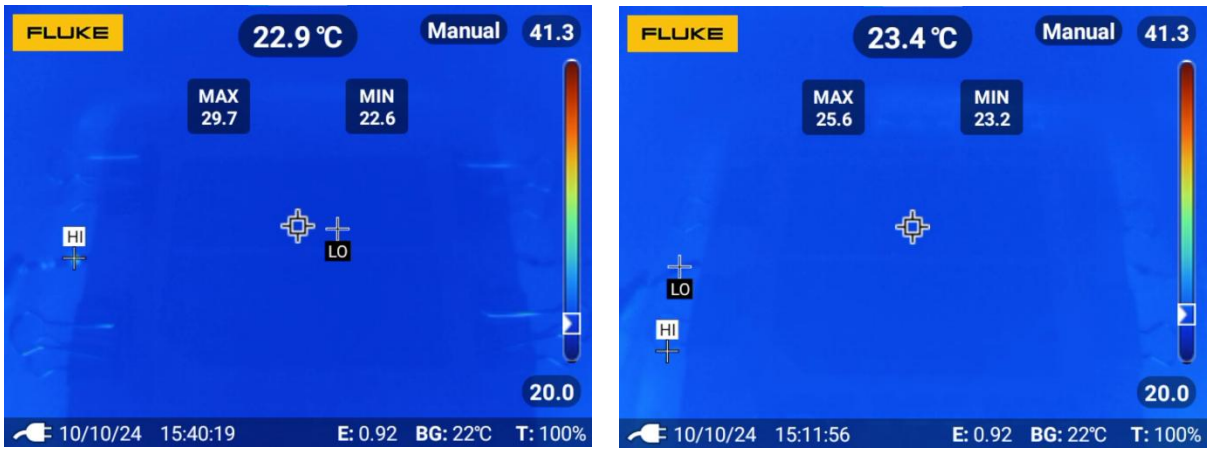

Figure 16. FLUKE capture at time 0 s of the reference sample (left) and the ILE sample (right)

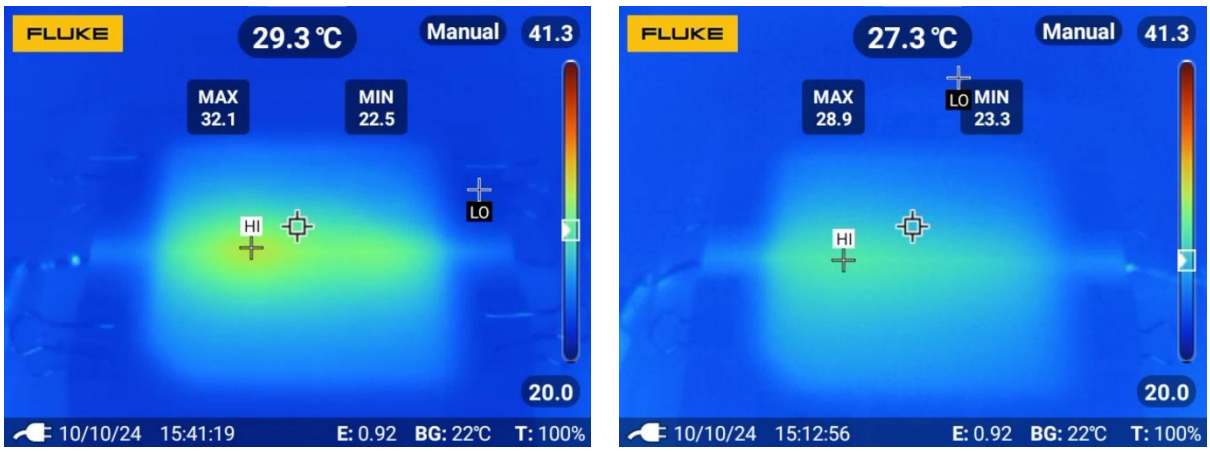

Figure 17. FLUKE capture at time 60 s of the reference sample (left) and the ILE sample (right)

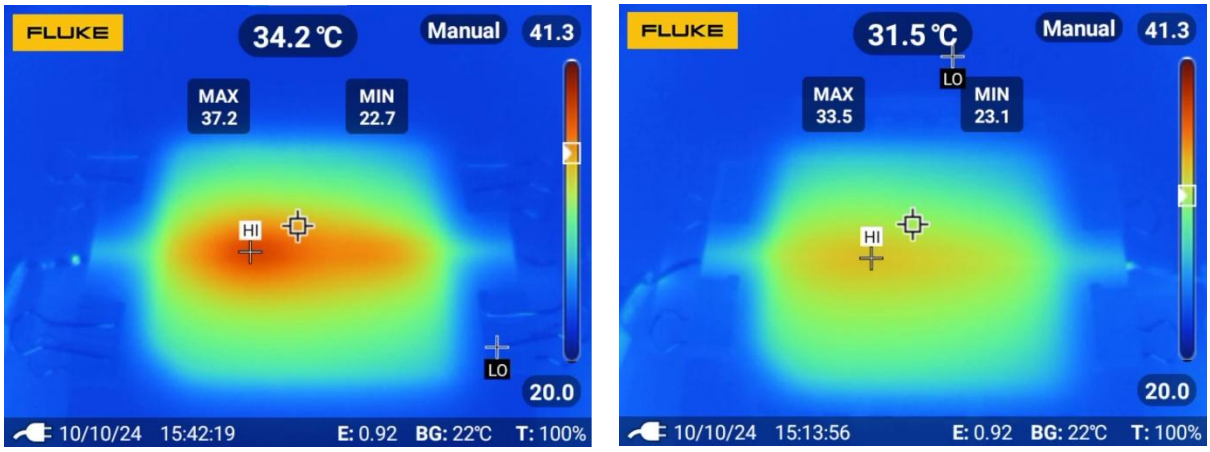

Figure 18. FLUKE capture at time 120 s of the reference sample (left) and the ILE sample (right)

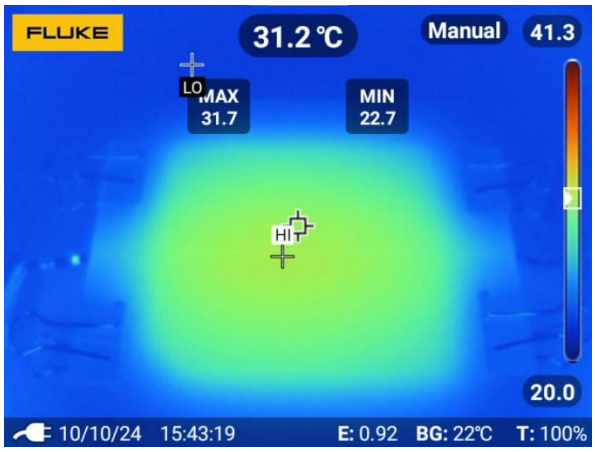

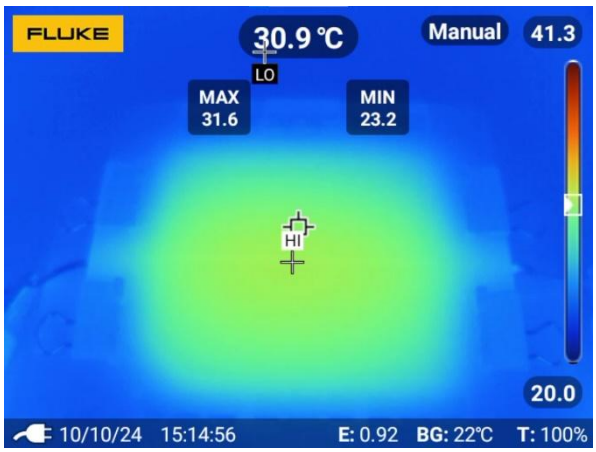

Figure 19. FLUKE capture at time 180 s of the reference sample (left) and the ILE sample (right)

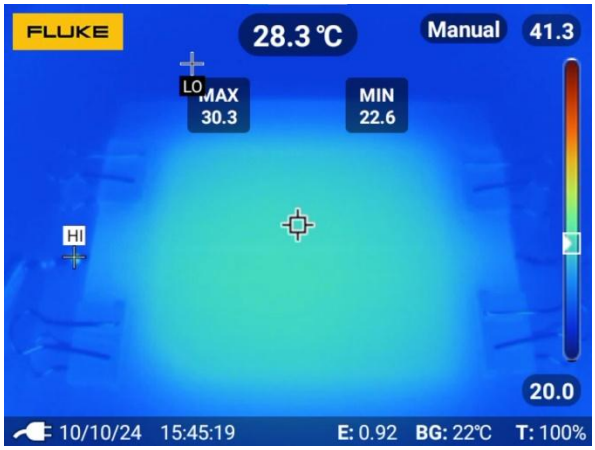

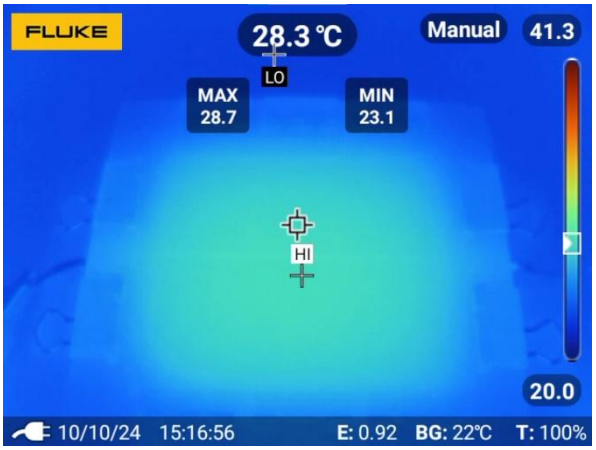

Figure 20. FLUKE capture at time 300 s of the reference sample (left) and the ILE sample (right)

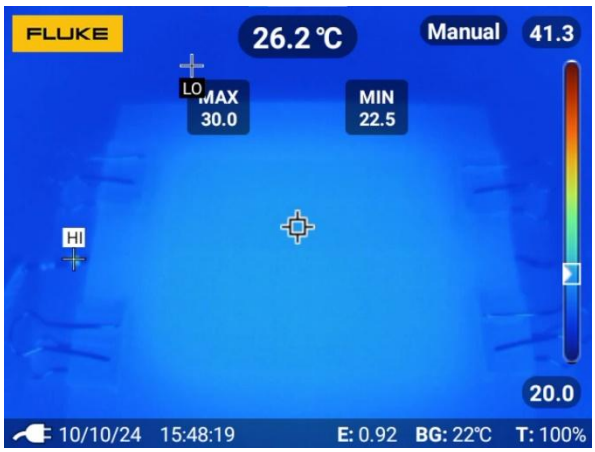

Figure 21. FLUKE capture at time 480 s of the reference sample (left) and the ILE sample (right)

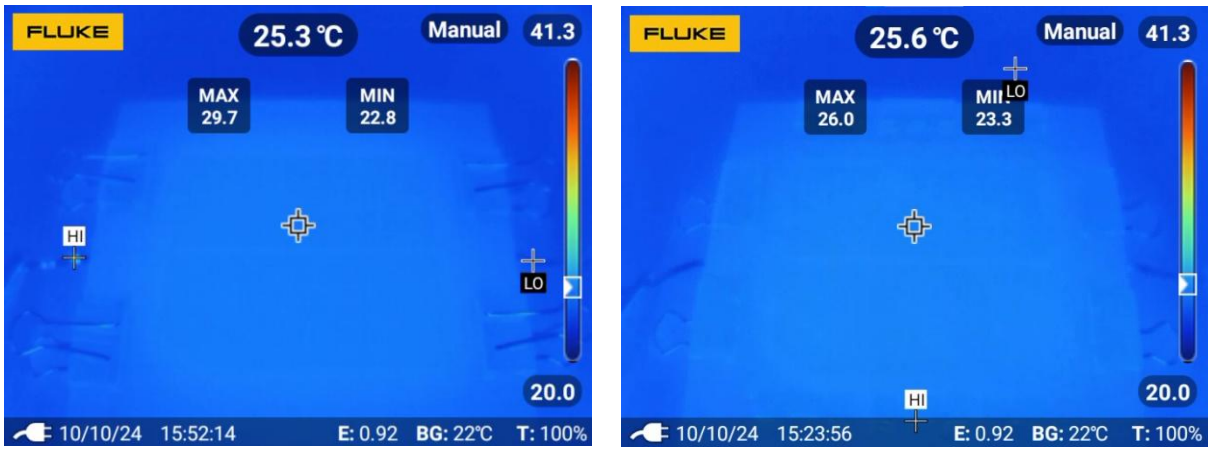

Figure 22. FLUKE capture at time 720 s of the reference sample (left) and the ILE sample (right)

When analyzing the results of the FLIR thermal imaging measurement, small but noticeable differences can be seen in the thermal performance of the cells. During the heating period, the reference cell reached both a higher spot and overall temperature. During the cooling period, the ILE exhibited similar performance as the reference cell. Especially the reduction on the maximum temperature point reinforces the idea behind the better temperature management qualities of ILE cell.

The measurement was repeated a couple of weeks later with new samples. The heating duration was also increased to 180 seconds. Consequently, the cooling time, here the FLIR imaging time, was also increased to 15 minutes. The following Figures, 23–30, show the results of this repeated experiment.

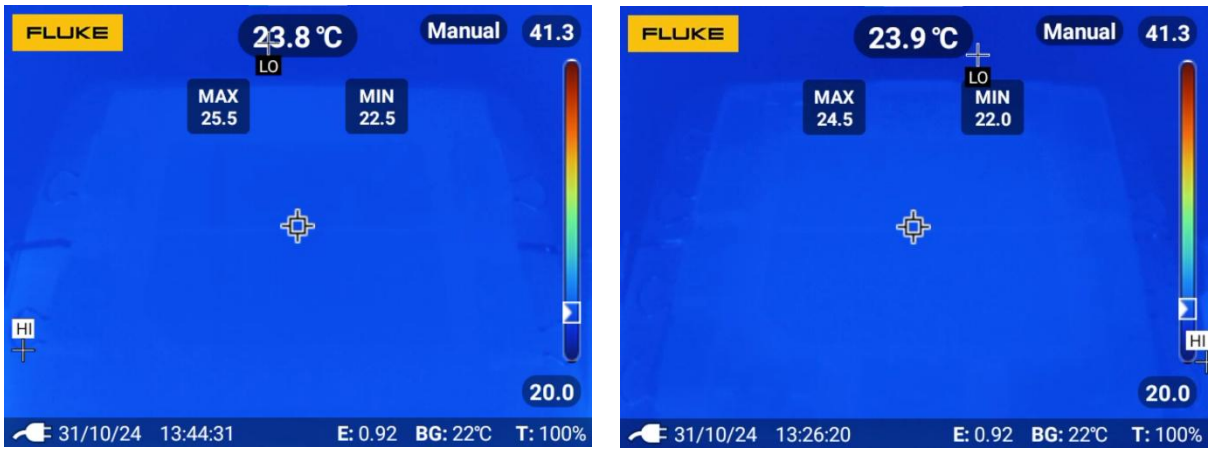

Figure 23. FLUKE capture at time 0 s of the reference sample 2 (left) and the ILE sample 2 (right)

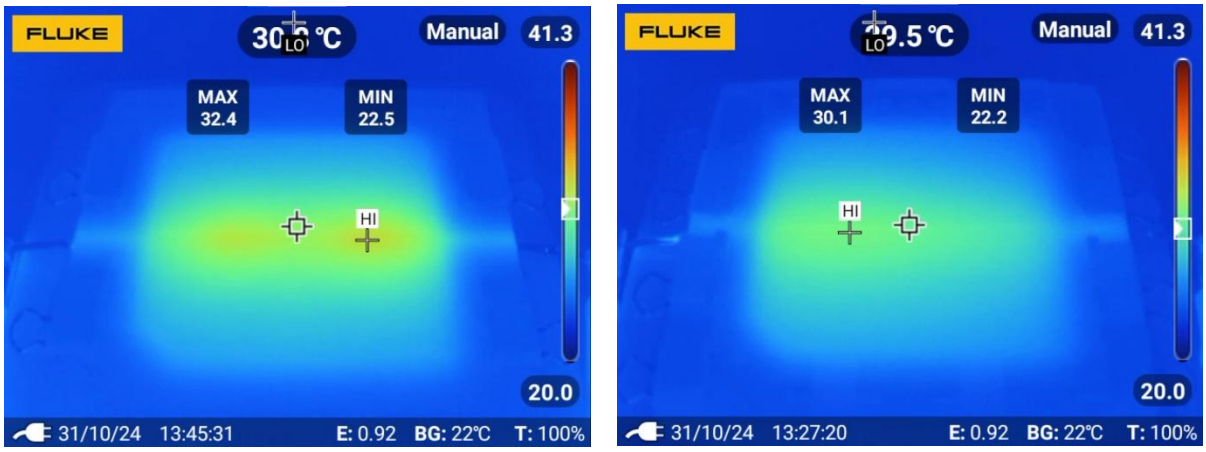

Figure 24. FLUKE capture at time 60 s of the reference sample 2 (left) and the ILE sample 2 (right)

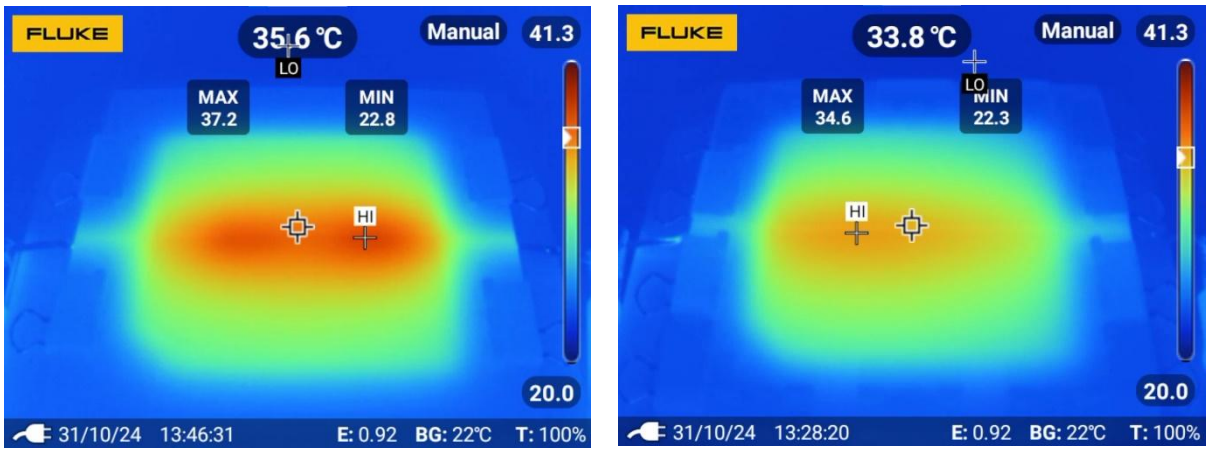

Figure 25. FLUKE capture at time 120 s of the reference sample 2 (left) and the ILE sample 2 (right)

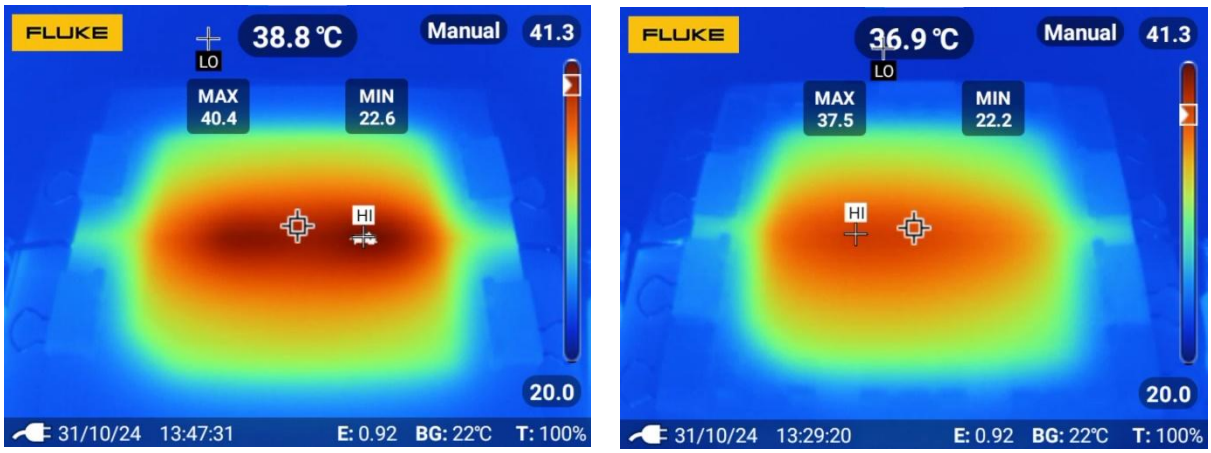

Figure 26. FLUKE capture at time 180 s of the reference sample (left) and the ILE sample (right)

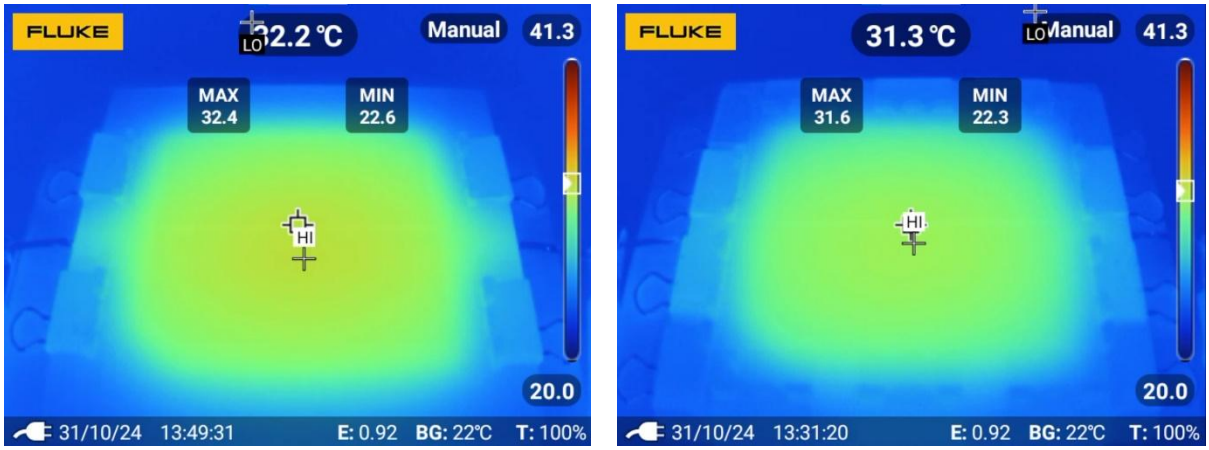

Figure 27. FLUKE capture at time 300 s of the reference sample (left) and the ILE sample (right)

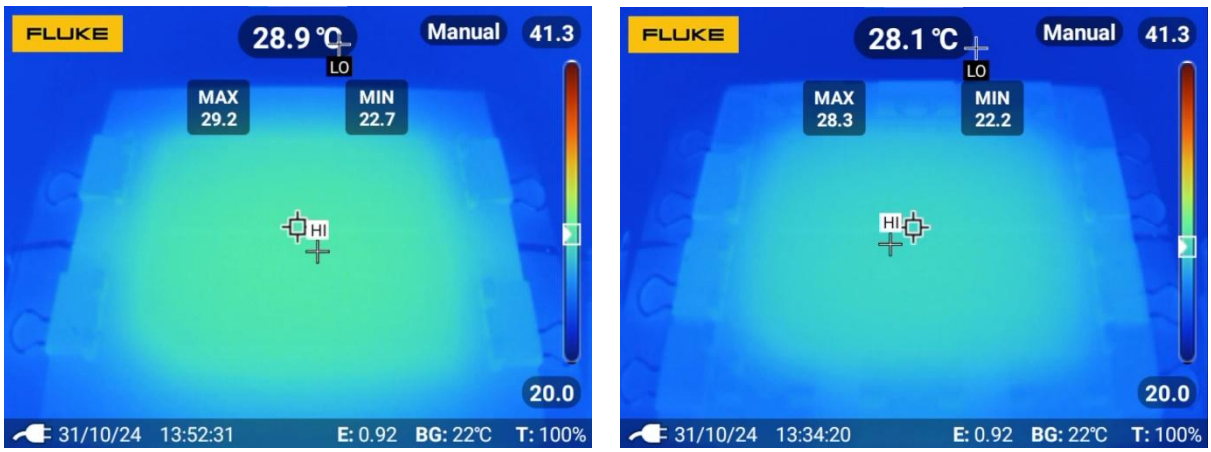

Figure 28. FLUKE capture at time 480 s of the reference sample (left) and the ILE sample (right)

Figure 29. FLUKE capture at time 720 s of the reference sample (left) and the ILE sample (right)

Figure 30. FLUKE capture at time 900 s of the reference sample (left) and the ILE sample (right)

By increasing the heating time, while using the same heating power, the temperature stabilizing effect of the ILE can be observed even more clearly. Here the reference cell reached much higher temperature values, even exceeding set maximum value of the temperature scale. This exceedance is visible as a white noisy point at Figure 26, HI-point on the right side of the left figure.

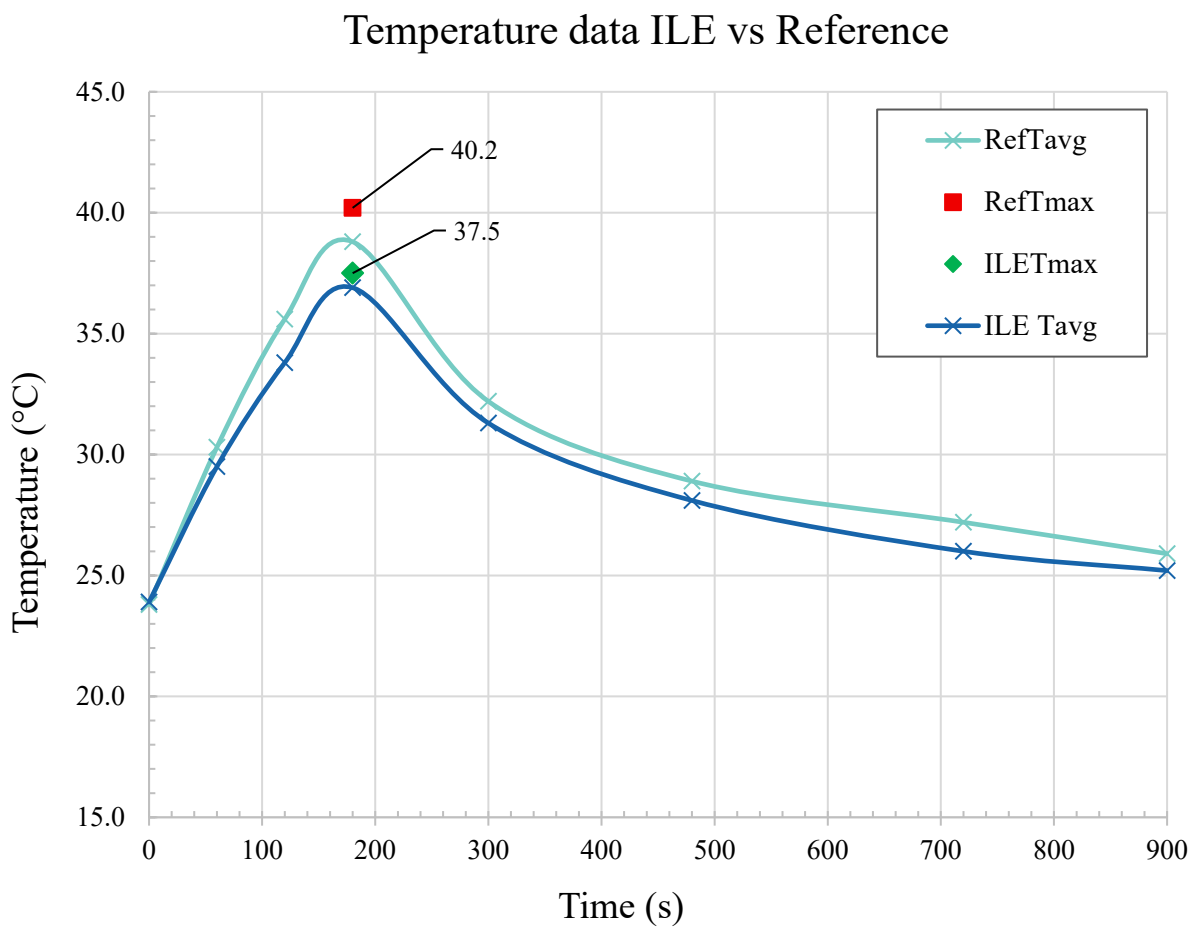

Figure 31. 2nd Thermal imaging-measurement data plotted with data points marked by "X"

Figure 31. shows the difference between the reference sample and ILE. Average temperature was plotted as well as the maximum temperature each sample achieved at 180 seconds. The graph is not an ideal method for visualizing the benefits of ILE as the uniformity is not visible. Otherwise, the heating and cooling curves are almost identical, although the reference cell achieved a higher maximum temperature.

5.3 Experimental Results – Recyclability

The recyclability of solar modules consists of multiple factors and is hard to quantify. For this thesis, recyclability was studied at a basic level. The main problem, the need for heat, and therefore energy, is eliminated when using ILE, as the encapsulant can be drained away and recycled as silicone oil or recycled by production of silicone polymers. All the other parts of the photovoltaic module will stay relatively untouched and can be recycled via their own paths. The aluminum frame can be recycled as aluminum; glass can for example be sold or recycled as needed. Potential polymer gaskets can be recycled via the recycling routes applicable to said polymer materials. The reduction of disassembly effort is extreme. From first-hand experience, the disassembling of a full-size commercial EVA encapsulated photovoltaic module requires force, time and effort. The disassembly of any of the prototype ILE modules requires less than a minute of time, and common tools such as a hex key or screwdriver. The most tested prototype edition, Prototype B, was the most easily disassembled, as the module is held together with spring steel clips. The spring steel clips can be slid off, with little force, and the encapsulant can be drained away. Afterwards each of the components can be separated as preferred. [26]

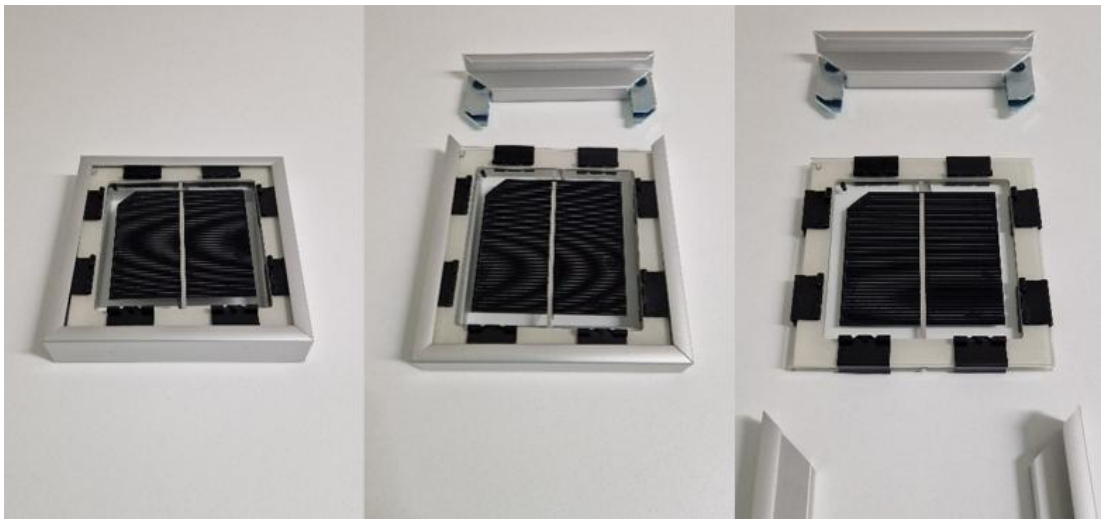

Figure 32. Disassembly of the protective frame

The disassembly process starts with removing the protective aluminum frame as shown in Figure 32. The process leaves the bare module held together with spring clips. The NBR gasket has good adhesion between the glass surfaces, and itself, hence, the spring clips used in this construction can be removed without the risk of the encapsulation leaking prematurely.

Figure 33. Draining of the encapsulant

The disassembly process can be continued by draining the encapsulant from the module as shown in Figure 33. On this prototype, the encapsulant can be drained simply by removing the plug from the hole on the top surface glass and the spring clips holding the module together. After this, the top glass can be removed and the process continued as pictured below in Figure 34.

Figure 34. Disassembled module with the wafer intact

After disassembly, each of the components can be reused or recycled as necessary. The most impactful factor when compared to other current solar module constructions, the wafer can be removed intact, and reused as is. Naturally, the other components also remain intact and reusable or recyclable: the glass, the strings and busbars and conditionally the gasket.

With the information gathered from the disassembly process, the ease of disassembly of ILE module can be compared with a common EVA encapsulated module. The method selected consisted of heating the module with a heat gun and trying to separate the components as shown in Figure 35. The process was not successful as the EVA acts as a strong adhesive by design. This meant that excessive heating was used, the glass shattered from thermal expansion but the module stood mostly intact. This demonstration shows the required effort of recycling current solar modules. And why solar cells are mostly recycled by mechanical or chemical efforts – grinding the module with all its components into minced solar module and separating the crushed mixed waste afterwards. The chemical method is under study but understandably requires chemicals, [26] in contrast to the simple disassembly of the ILE-module, whose recycling process is effortless.

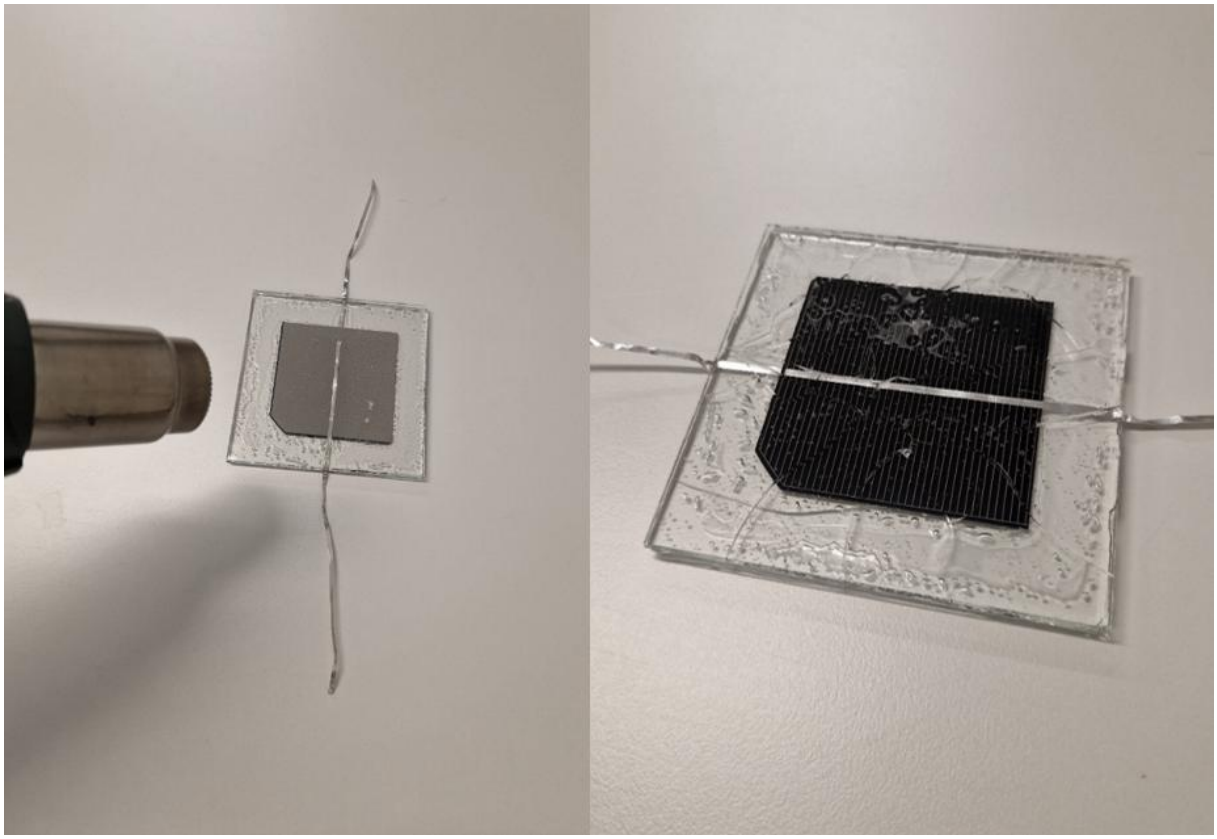

Figure 35. The disassembly of the reference cell; heating and aftermath.

5.4 Experimental Results – Materials

During the prototyping phase, some possible gasket materials were selected for immersion testing in the chosen liquid. These materials remained immersed in dimethylpolysiloxane for 16 months at room temperature as pictured in Figure 36. The selected gasket materials were NBR, Silicone, food grade NBR and EPDM. The materials did not exhibit any visible interactions with the liquid, except with common, black-colored NBR. With this material, visible discoloration of the liquid occurred. This, however, was expected, given the experience of the preliminary testing. The gasket used in the preliminary testing was cut NBR sheet. The surface of the cut was the most likely culprit for the discoloration. For the material immersion testing, the sample chosen was a set length of NBR O-ring material. This sample had only two cut surfaces with diameters of 2 mm, and therefore the amount of discoloration was extremely limited. The discoloration is likely due to the leaching of additives like antioxidants or UV stabilizers from the NBR material. NBR is manufactured for a wide range of applications. Some applications, such as use in food-safe applications, require higher standards to limit the exposure for additives. The food grade NBR was chosen for this series of experiments, and it performed without observed issues. Therefore, I would recommend using food-grade gasket materials in further studies. [35]

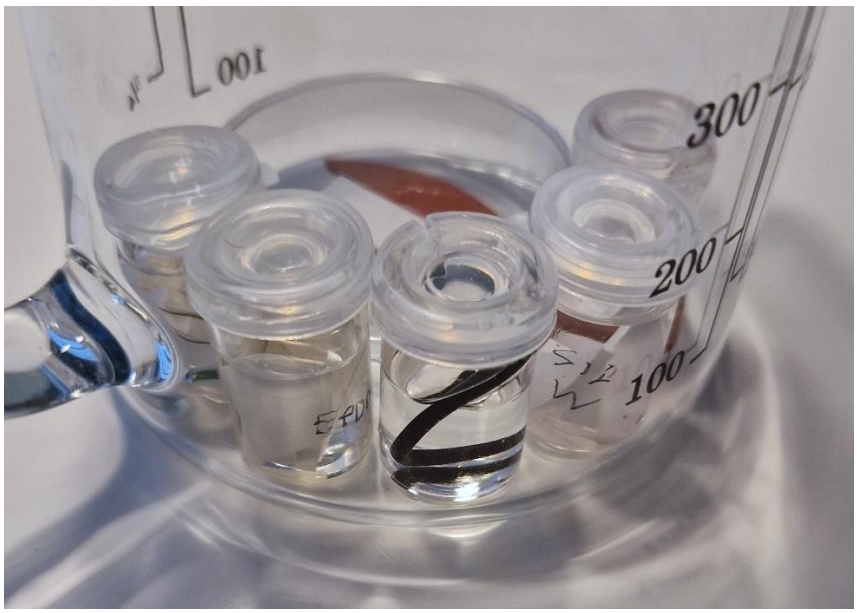

Figure 36. Gasket samples immersed in dimethylpolysiloxane 14.6.2023

From the samples immersed in dimethylpolysiloxane for 16 months, visually only the NBR sample can be seen to exhibit discoloration. All other samples have liquids comparable to new clear dimethylpolysiloxane. The true color of the liquid can be most easily seen when separated into a separate container with a white background. As seen in figure 37, the color of the liquid appears reddish, but this is only due to scattering from the colored silicone pieces.

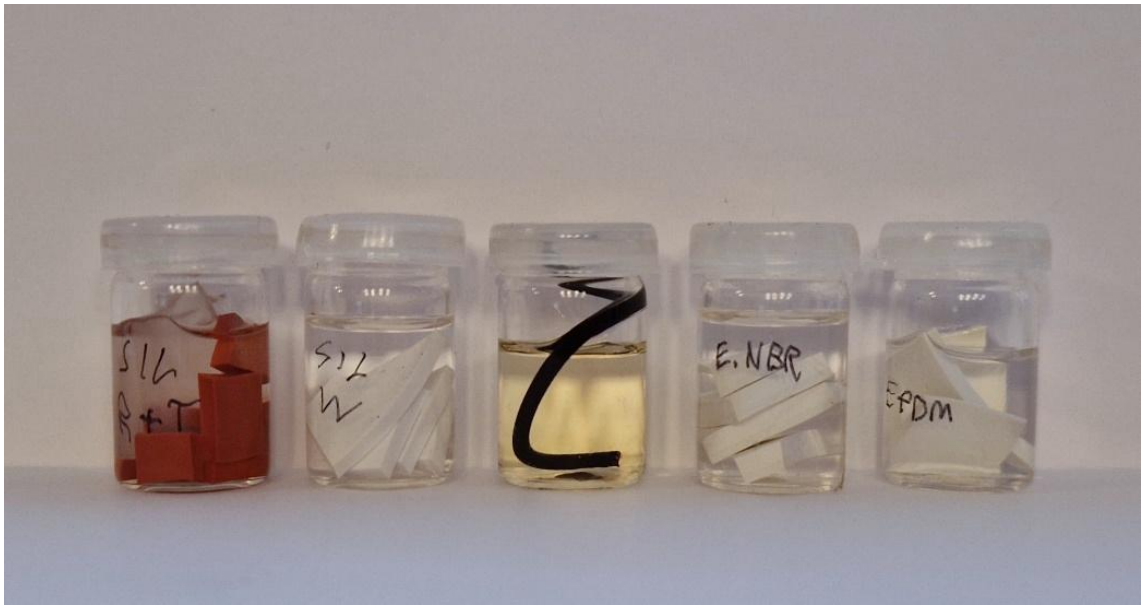

Figure 37. Immersed gasket samples after 16 months, note the discoloration of the center sample. From left to right: Silicone (red and transparent), Silicone (white), NBR, Food grade NBR, EPDM. 15.10.2024

6 Discussion

6.1 Interpretation

The visual observation done at each outdoor experiment phase showed no visual degradation or discoloration of either the cell, or the encapsulation. Likewise, the performance of the cell remained unchanged during the testing period. Hence, the outdoor experiment proposes that ILE is a viable method for encapsulation based on limited time outdoor testing in rough northern conditions.

The thermal performance of ILE is probably due to the liquid nature of the encapsulant. Thermal energy can spread via thermal convection, here the liquid is moving away from the heat source and therefore drawing cooler liquid into the area. This simple physical explanation underlines the benefits of inert liquid encapsulation. With common encapsulants, like EVA, the energy is transferred without the benefit of convection.

The disassembly process required considerably less effort when comparing ILE to the reference cell assembled using vacuum lamination process. Importantly, all separated components remained intact therefore facilitating easier recycling or reuse.

6.2 Limitations

Given the scope of this thesis, the experimental setups were relatively simple. The feasibility of each prototype as a commercial unit was not in any way considered as the economic aspect was outside the scope of this project. The main outdoor aging test had limitations on the experimental setup, the accuracy of the results cannot be guaranteed, as the experiment included numerous variables, and the measurement accuracy was not perfect. Noteworthy, the experimental time constraints might have affected the outcome. The prototypes were constructed for experimental use only, and do not in any way present a viable solution for commercial market. In current photovoltaic modules, encapsulation acts as a binding agent for structural stability for the module. This is not possible with the ILE module and this needs to be accounted for. The thermal experiment gave partly inconclusive results, and these should be repeated. The primary goal, however, was achieved, as the feasibility of this encapsulation method was successfully demonstrated.

6.3 Future Research

The main purpose of this study was to determine whether this type of solar cell construction could be a viable method. Therefore, the scope of this thesis was limited, however, the results support the concept and future research on inert liquid encapsulation.

This thesis focused on one single promising material. Future research should include other possible materials for inert liquid encapsulation. My recommendation is to also include the economic aspects, costs, and overall feasibility of the concept while considering the possibility of highly specialized use scenarios, such as aerospace applications. My last recommendation would be to increase the sample size and include more advanced measurement techniques and experimental setups.

6.3.1 Passive Daytime Radiative Cooling

Passive daytime radiative cooling (PDRC) uses the high emissivity of materials to cool surfaces without external effort. Materials applicable have high emissivity at longwave infrared (LWIR), where the infrared window on earth's atmosphere can be utilized for heat transfer into space. The liquid encapsulation material chosen, dimethylpolysiloxane, is one of the most used PDRC materials. Dimethylpolysiloxane has been used for passive daytime radiative cooling due to its high longwave infrared emissivity. One possible application would be to utilize the possible cooling effect during nights, when solar radiation won't affect the module temperature. Passive radiative cooling application, day or night, remains purely hypothetical and is not examined further in the scope of this thesis. [36]

7 Conclusion

Real-life outdoor aging experiment of silicon solar cells encapsulated in inert liquid encapsulation showed no evidence of performance degradation. The concept appears to be viable. The outdoor experiment was conducted under great environmental changes and thus highlights the potential for extreme-environment applications.

According to the results gathered from the thermal performance analysis, the thermal performance of ILE modules was the same or better than that of the common modules using EVA encapsulation materials.

Using qualitative analysis and disassembly testing, the overall recyclability of the ILE cells was determined to be better than that of conventional solar cells. The disassembly of the module was considerably easier, and significant benefits regarding the time used, and other necessary conditions comparing to those of current conventional modules, were visible. Notably the elimination of the need for external heat, and/or chemicals for the disassembly are highly beneficial for the recycling process. With the modular design possibilities, the purification or replacement of the encapsulant poses significant improvement for the environmental impact of the solar module. As the module can be “renewed”, instead of discarding and recycling the otherwise working module.

Considering only the technical side of the ILE module, the module has potential applications almost everywhere, where conventional silicon solar modules are used. Highest potential might be with large- to medium-scale solar farms, and private use where the potential increase in lifetime is valued, and therefore the potentially higher overall cost can be justified. Notably the easier recycling, and even more so the potential for renewing, might have a positive impact on the attitude towards these solar modules, as ILE modules might be seen as a more environmentally conscious choice.

8 References

[1] S. Ebnesajjad and A. H. Landrock, “Characteristics of Adhesive Materials,” in *Adhesives Technology Handbook*, Elsevier, 2015, pp. 84–159. doi: 10.1016/B978-0-323-35595-7.00005-X.

[2] K. Aitola *et al.*, “Encapsulation of commercial and emerging solar cells with focus on perovskite solar cells,” *Solar Energy*, vol. 237, pp. 264–283, May 2022, doi: 10.1016/j.solener.2022.03.060.

[3] A. K. Schnatmann, F. Schoden, and E. Schwenzfeier-Hellkamp, “Sustainable PV Module Design—Review of State-of-the-Art Encapsulation Methods,” *Sustainability*, vol. 14, no. 16, p. 9971, Aug. 2022, doi: 10.3390/su14169971.

[4] A. Divya, T. Adish, P. Kaustubh, and P. S. Zade, “Review on recycling of solar modules/panels,” *Solar Energy Materials and Solar Cells*, vol. 253, p. 112151, May 2023, doi: 10.1016/j.solmat.2022.112151.

[5] W. D. Callister and D. G. Rethwisch, *Materials science and engineering*, 9. ed., SI version. Hoboken, NJ: Wiley, 2015.

[6] M. D. Kempe, G. J. Jorgensen, K. M. Terwilliger, T. J. McMahon, C. E. Kennedy, and T. T. Borek, “Acetic acid production and glass transition concerns with ethylene-vinyl acetate used in photovoltaic devices,” *Solar Energy Materials and Solar Cells*, vol. 91, no. 4, pp. 315–329, Feb. 2007, doi: 10.1016/j.solmat.2006.10.009.

[7] L.-M. Huang, S. H.-Y. Hsu, R.-C. Lai, F.-M. Lin, C.-Y. Peng, and F.-Y. Yeh, “Physical Properties of EVA and PVB Encapsulant Materials for Thin Film Photovoltaic Module Applications,” Sep. 2008.

[8] F. Toniolo *et al.*, “Efficient and reliable encapsulation for perovskite/silicon tandem solar modules,” *Nanoscale*, vol. 15, no. 42, pp. 16984–16991, 2023, doi: 10.1039/D2NR06873G.

[9] N. T. Dintcheva, E. Morici, and C. Colletti, “Encapsulant Materials and Their Adoption in Photovoltaic Modules: A Brief Review,” *Sustainability*, vol. 15, no. 12, Art. no. 12, Jan. 2023, doi: 10.3390/su15129453.

[10] G. Beaucarne, A. Dupont, D. Puthenmadom, N. Shephard, and T. Sample, “Material study of photovoltaic modules with silicone encapsulation after long-term outdoor exposure,” *Solar Energy Materials and Solar Cells*, vol. 230, p. 111298, Sep. 2021, doi: 10.1016/j.solmat.2021.111298.

[11] M. A. Green and M. J. Keevers, “Optical properties of intrinsic silicon at 300 K,” *Progress in Photovoltaics*, vol. 3, no. 3, pp. 189–192, Jan. 1995, doi: 10.1002/pip.4670030303.

[12] B. K. Mousavi, A. K. Mousavu, T. Busani, M. H. Zadeh, and S. R. J. Brueck, “Nanostructured Anti-Reflection Coatings for Enhancing Transmission of Light,” *JAMP*, vol. 07, no. 12, pp. 3083–3100, 2019, doi: 10.4236/jamp.2019.712217.

[13] “Methyl Phenyl Polysiloxane TPD-255.” Accessed: Jul. 16, 2024. [Online]. Available: https://www.topsilicone.com/product/phenyl-methyl-silicone-oil-tpd-255

[14] “Silicone Diffusion Pump Oil TOPDA 705 | DC 705 Replacement.” Accessed: Jul. 16, 2024. [Online]. Available: https://www.topsilicone.com/product/silicone-diffusion-pump-oil-topda-705

[15] A. A. Q. Hasan *et al.*, “A review on silicon photovoltaic module degradations and recent identification techniques,” *Solar Energy*, vol. 288, p. 113288, Mar. 2025, doi: 10.1016/j.solener.2025.113288.

[16] P. A. Klonos, “Crystallization, glass transition, and molecular dynamics in PDMS of low molecular weights: A calorimetric and dielectric study,” *Polymer*, vol. 159, pp. 169–180, Dec. 2018, doi: 10.1016/j.polymer.2018.11.028.

[17] A. A. Q. Hasan, A. Ahmed Alkahtani, S. A. Shahahmadi, M. Nur E. Alam, M. A. Islam, and N. Amin, "Delamination-and Electromigration-Related Failures in Solar Panels—A Review," *Sustainability*, vol. 13, no. 12, p. 6882, Jun. 2021, doi: 10.3390/su13126882.

[18] B. Zhang *et al.*, "Dielectric Properties Characterization and Evaluation of Commercial Silicone Gels for High-Voltage High-Power Power Electronics Module Packaging," *IEEE Trans. Dielect. Electr. Insul.*, vol. 30, no. 1, pp. 210–219, Feb. 2023, doi: 10.1109/TDEI.2022.3225247.

[19] A. Virtuani, E. Annigoni, and C. Ballif, "One-type-fits-all-systems: Strategies for preventing potential-induced degradation in crystalline silicon solar photovoltaic modules," *Progress in Photovoltaics*, vol. 27, no. 1, pp. 13–21, Jan. 2019, doi: 10.1002/pip.3066.

[20] "Dimethicone | 9006-65-9." Accessed: May 04, 2025. [Online]. Available: https://www.chemicalbook.com/ChemicalProductProperty_EN_CB0696472.htm

[21] "What is a Dielectric Constant and DF of Plastic Materials?" Accessed: May 04, 2025. [Online]. Available: https://passive-components.eu/what-is-dielectric-constant-of-plastic-materials/

[22] B. Bora *et al.*, "Accelerated stress testing of potential induced degradation susceptibility of PV modules under different climatic conditions," *Solar Energy*, vol. 223, pp. 158–167, Jul. 2021, doi: 10.1016/j.solener.2021.05.020.

[23] U. Weber *et al.*, "Acetic Acid Production, Migration and Corrosion Effects in Ethylene-Vinyl-Acetate- (EVA-) Based PV Modules," *27th European Photovoltaic Solar Energy Conference and Exhibition; 2992-2995*, p. 4 pages, 2730 kb, 2012, doi: 10.4229/27THEUPVSEC2012-4CO.9.4.

[24] "Natural Convection: Understanding Heat Transfer in Fluid Systems | CFDLAND." Accessed: Feb. 23, 2026. [Online]. Available: https://cfdland.com/natural-convection-understanding-heat-transfer-in-fluid-systems/

[25] J. Lee, N. Duffy, and J. Allen, "A Review of End-of-Life Silicon Solar Photovoltaic Modules and the Potential for Electrochemical Recycling," *Adv Energy and Sustain Res*, vol. 6, no. 2, p. 2400254, Feb. 2025, doi: 10.1002/aesr.202400254.

[26] S. Weckend, A. Wade, and G. Heath, "End of Life Management: Solar Photovoltaic Panels," NREL/TP--6A20-73852, T12-06:2016, 1561525, Jun. 2016. doi: 10.2172/1561525.

[27] L.-E. Perret-Aebi , H.-Y. Li , R. Théron, G. Roeder, Y. Luo, T. Turlings, R. F. M. Lange , C. Ballif, "INSIGHTS ON EVA LAMINATION PROCESS: WHERE DO THE BUBBLES COME FROM?," presented at the 25th European Photovoltaic Solar Energy Conference and Exhibition, Valencia, Spain.

[28] R. Ramli, N. Chee Mang, Z. Ahmad, M. Jaafar, and M. R. R. Mohd Arif Zainol, "Synthesis and Studies on the Effect of Phenyl Side – Chain Content on Refractive Index of Polysiloxane Resin," *AMM*, vol. 754–755, pp. 881–885, Apr. 2015, doi: 10.4028/www.scientific.net/AMM.754-755.881.

[29] D. H. W. Steel, D. Wong, and T. Sakamoto, "Silicone oils compared and found wanting," *Graefes Arch Clin Exp Ophthalmol*, vol. 259, no. 1, pp. 11–12, Jan. 2021, doi: 10.1007/s00417-020-04810-9.

[30] PubChem, "Dimethicone." Accessed: Sep. 25, 2024. [Online]. Available: https://pubchem.ncbi.nlm.nih.gov/compound/Dimethicone

[31] "Download observations - Finnish Meteorological Institute." Accessed: Jun. 11, 2025. [Online]. Available: https://en.ilmatieteenlaitos.fi/download-observations

[32] J. Allan, H. Pinder, and Z. Dehouche, “Enhancing the thermal conductivity of ethylene-vinyl acetate (EVA) in a photovoltaic thermal collector,” *AIP Advances*, vol. 6, no. 3, p. 035011, Mar. 2016, doi: 10.1063/1.4944557.
[33] J. E. Mark, Ed., *Polymer Data Handbook: Second Edition*. Oxford University PressNew York, NY, 2009. doi: 10.1093/oso/9780195181012.001.0001.
[34] M. P. Belançon, M. Sandrini, V. S. Zanuto, and R. F. Muniz, “Glassy materials for Silicon-based solar panels: Present and future,” *Journal of Non-Crystalline Solids*, vol. 619, p. 122548, Nov. 2023, doi: 10.1016/j.jnoncrysol.2023.122548.
[35] L. W. McKeen, *The effect of UV light and weather on plastics and elastomers*, Fourth edition. in Plastics design library. Amsterdam: Elsevier, 2019.
[36] L. Li *et al.*, “Advanced passive daytime radiative cooling: from material selection and structural design to application towards multifunctional integration,” *Adv Compos Hybrid Mater*, vol. 8, no. 1, p. 97, Dec. 2024, doi: 10.1007/s42114-024-01127-7.

Appendices

Appendix 1 – Unprocessed IV-curve S1

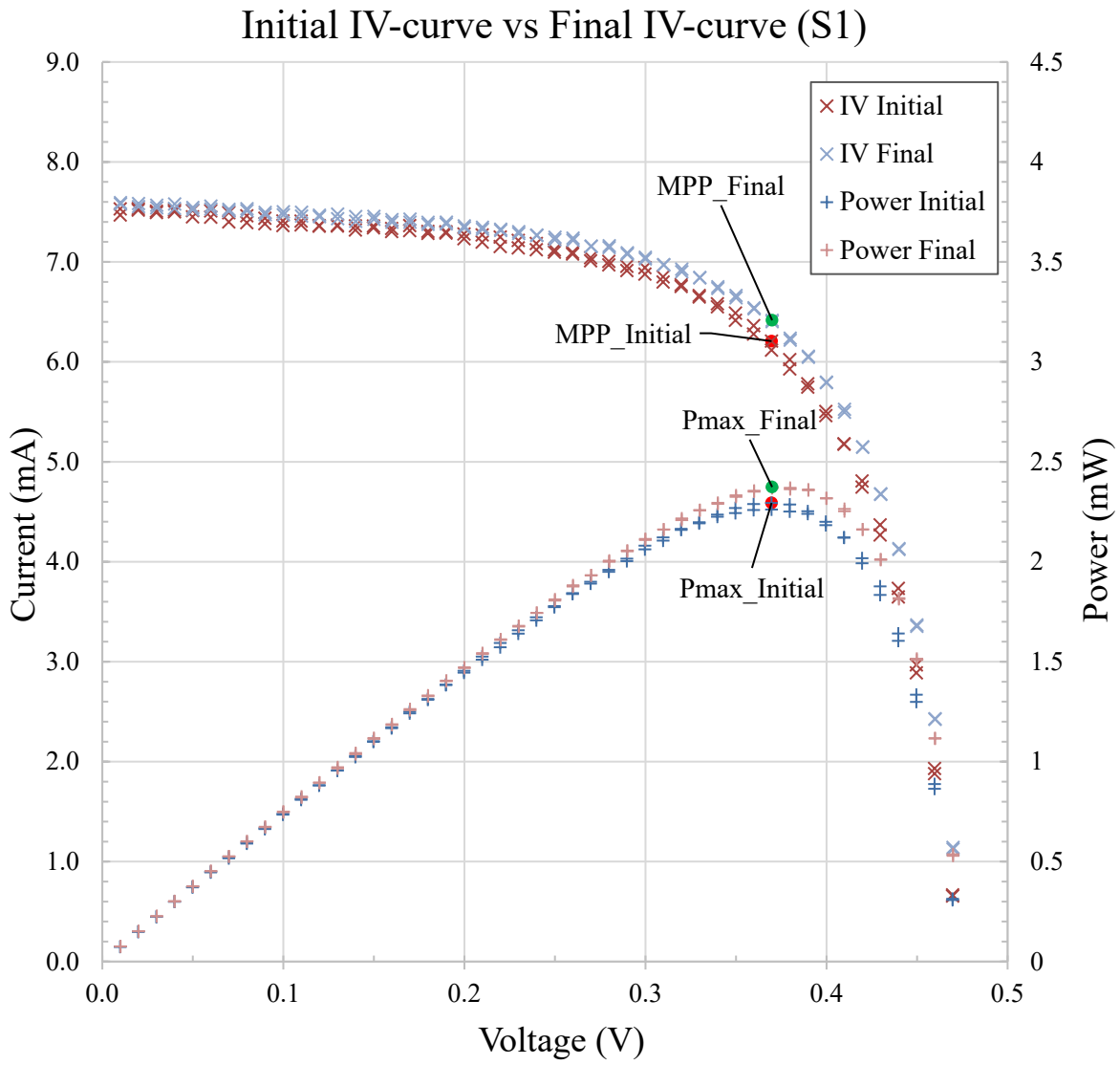

A 1. Unprocessed graph with raw datapoints

Appendix 2 – Unprocessed IV-curve S2

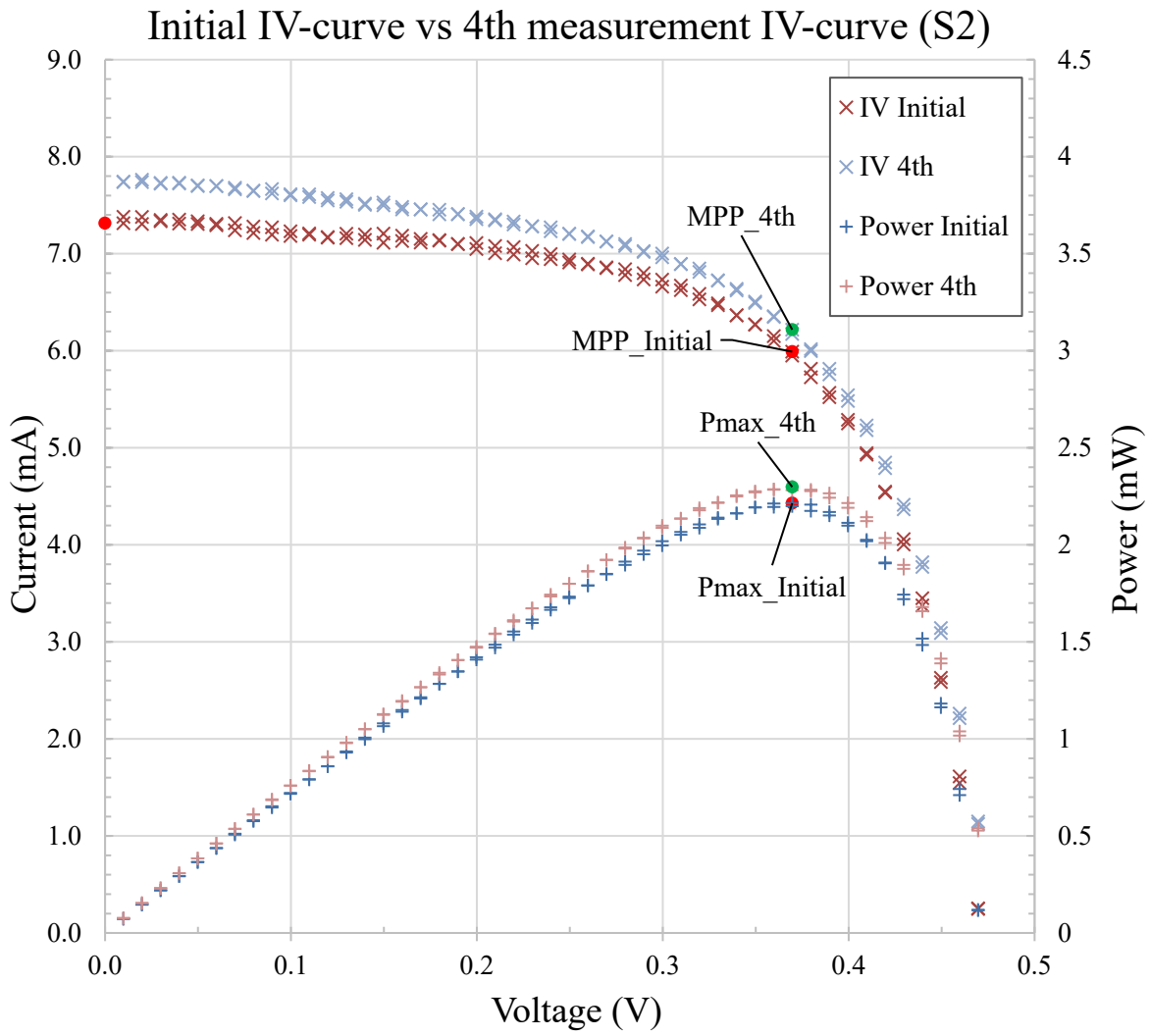

A 2. Unprocessed graph with raw datapoints